CAPITAL UNIVERSITY OF SCIENCE AND TECHNOLOGY, ISLAMABAD

Impact of Tangent Hyperbolic Fluid and Chemical Reaction on Radiative MHD Flow

by

Usman Khaliq

A thesis submitted in partial fulfillment for the
degree of Master of Philosophy

in the
Faculty of Computing
Department of Mathematics

2021

Copyright © 2021 by Usman Khaliq

*I dedicate this Sincere effort to my **Family**, my dear **Parents**, my elegant **Teachers**, and my Supervisor **Dr. Shafqat Hussain** who are always source of Inspiration for me and their contributions are uncounted.*

CERTIFICATE OF APPROVAL

Impact of Tangent Hyperbolic Fluid and Chemical Reaction on Radiative MHD Flow

by

Usman Khaliq

(MMT191006)

THESIS EXAMINING COMMITTEE

S. No.	Examiner	Name	Organization
(a)	External Examiner	Dr. Bilal Ashraf	COMSATS, Islamabad
(b)	Internal Examiner	Dr. Abdul Rehman Kashif	CUST, Islamabad
(c)	Supervisor	Dr. Shafqat Hussain	CUST, Islamabad

_____

Dr. Shafqat Hussain

Thesis Supervisor

November, 2021

_____

Dr. Muhammad Sagheer

Head

Dept. of Mathematics

November, 2021

_____

Dr. Muhammad Abdul Qadir

Dean

Faculty of Computing

November, 2021

Author's Declaration

I, **Usman Khaliq** hereby state that my MPhil thesis titled "**Impact of Tangent Hyperbolic Fluid and Chemical Reaction with on Radiative MHD Flow**" is my own work and has not been submitted previously by me for taking any degree from Capital University of Science and Technology, Islamabad or anywhere else in the country/abroad.

At any time if my statement is found to be incorrect even after my graduation, the University has the right to withdraw my MPhil Degree.

(Usman Khaliq)

Registration No: MMT191006

Plagiarism Undertaking

I solemnly declare that research work presented in this thesis titled "**Impact of Tangent Hyperbolic Fluid and Chemical reaction with on Radiative MHD Flow**" is solely my research work with no significant contribution from any other person. Small contribution/help wherever taken has been duly acknowledged and that complete thesis has been written by me.

I understand the zero tolerance policy of the HEC and Capital University of Science and Technology towards plagiarism. Therefore, I as an author of the above titled thesis declare that no portion of my thesis has been plagiarized and any material used as reference is properly referred/cited.

I undertake that if I am found guilty of any formal plagiarism in the above titled thesis even after award of MPhil Degree, the University reserves the right to withdraw/revoke my MPhil degree and that HEC and the University have the right to publish my name on the HEC/University website on which names of students are placed who submitted plagiarized work.

(Usman Khaliq)

Registration No: MMT191006

Acknowledgement

All Praises belong to Almighty Allah, Lord and the Creator of the universe Who bestowed upon me the courage and His countless blessing enabled me to accomplish my MPhil Studies. He is the Most Powerful, Gracious, and Beneficent. All respect to our Holy prophet Muhammad (peace be upon him) who enables us to recognize our creator Allah, and who is forever a torch of guidance for the whole mankind. My heartiest gratitude is to my respected supervisor **Dr. Shafqat Hussain** for invaluable and inspiring guidance and encouraging discussions which enabled me to complete my work successfully. His encouraging and instructive behavior always motivated me to implement new ideas in my research work. May Allah blesses him with best. In fact, it is a matter of pride and privilege for me to be his MPhil student. Thanks, also due to my chairman, Department of Mathematics Capital University of Science and Technology for providing necessary research facilities. I am highly indebted to my respectable teachers for their guidance during my course work. I am proud of my friends and colleagues and My heartfelt thanks to my class fellows **Komal, Iffat** for always being there and bearing with me during the good and bad times during my wonderful days of MPhil My special words of gratitude to them for all his professional help that he has extended to me throughout. Finally, I wish to thank my **family** members for continuous support, inspiration, and encouragement, without whom I would never finish this thesis. My thanks go to my parents for the confidence and their love during all these years.

(Usman Khaliq)

Abstract

This investigation is undertaken to explore the impact of tangent hyperbolic fluid model and chemical reaction on the Magnetohydrodynamic laminar, incompressible two dimensional steady flow through a stretching surface. A mathematical model that resembles the physical flow problem has been developed. The proposed problem is modeled as a system of non-linear partial differential equations describing the conservation laws of mass, momentum and energy. Meanwhile, a system of non-linear ordinary differential equations are obtained by using appropriate similarity transformation on the governing partial differential equations. The resulting system of ordinary differential equations is solved numerically by utilizing a shooting technique coupled with Runge-Kutta method of order four, implemented in the computational software MATLAB. Influence of different physical parameters on velocity, temperature and concentration profiles are analyzed through graphs and tables. Numerical values of skin fraction coefficient, Nusselt number, and Sherwood number are also computed and analyzed.

Contents

List of Figures

List of Tables

Abbreviations

BVP   Boundary value problem

IVP   Initial value problem

MHD   Magnetohydrodynamics

ODEs   Ordinary differential equations

PDEs   Partial differential equations

RK   Runge-Kutta

Symbols

B_0 magnetic field strength

c proportionality constant

C_p specific heat at constant pressure

C_f skin friction coefficient

Ec Eckert number

k thermal conductivity

k^* mean absorption coefficient

K_p permeability of porous medium

M magnetic parameter

n power law index

Nu_x Nusselt number

Pr Prandtl number

Q heat generation parameter

Q_0 heat source coefficient

q_r radiative heat flux

q_w wall heat flux

R radiation parameter

r chemical reaction parameter

S suction and injection parameter

Sc Schmidt number

Sh_x Sherwood number

T fluid temperature

u, v velocity components in x and y directions

v_0 velocity of suction and injection

We Weissenberg number

x, y axial and normal coordinates

ρ density of the fluid

σ electrical conductivity

ν kinematic viscosity

μ co-efficient of fluid viscosity

σ^* Stefan-Boltzman constant

ξ similarity variable

λ permeability parameter

Chapter 1

Introduction

Different analysts have conducted comprehensive investigation on 2D boundary layer flow and heat exchange over a permeable extending sheet in the existence of magnetic field. Because of their broad utilization in different areas such as permeable heat exchangers, plasma studies solidification due to atomic reactor cooling, and filtration forms.

Magnetohydrodynamics is a field of mechanics that studies the magnetic characteristics and behaviour of electrically conducting fluids. A conducting fluid produces current when it passes through a magnetic field, as a result Lorentz force is created which changes the movement of the fluid. The MHD factor is essential in managing the cooling rate and for the obtaining the product's desired properties.

It is of concern that applications of MHD flows occur in a variety of fields of manufacturing, such as electrical propulsion for space travel, crystal development in liquids, fusion reactor cooling, etc. The numerical results of MHD flow in permeable media were obtained by Mcwhirter et al. [1]. Pavlov [2] was the first who studied the MHD flow over a stretched wall. Geindreau and Auriatlt [3] studied the tensorial filtration law in a inflexible permeable material under the impact of a magnetic field with Beavers-Joseph boundary conditions.

The effect of a magnetic field on fluid flow past a porous surface was investigated by Jat and Chaudhary [4]. As the porosity parameter increases, so does skin friction

and the coupling stress coefficient rises, according to Modather et al. [5]. In the flow section, there is a magnetic field, Das et al. [6] detailed on nanofluid stream through an oscillating permeable level plate. Viscous dissipation and Joule heating abstraction take part in many field like geophysical flow and nuclear engineering. The Joule heating effect on MHD free convection flow from a vertical flat plate was studied by Alim et al. [7]. Using Hall and ion-slip currents, Eldahab and Aziz [8] investigated the impact of viscous dissipation and Joule heating on MHD-free convection flow across a semi-infinite vertical flat plate.

The Hiemenz flow of a micropolar fluid was studied by Amin and Mohammadein [9]. Ali et al. [10] explored the MHD conjugate flow across a vertical plate. They presented how the physical quantities behave against flow govern parameters. Hakeem et al. [11] discussed the mass and heat exchanges, as well as heat absorption, magnetic field and velocity slips are all affected by viscous and Ohmic dissipation. The nature of MHD free convection flow across a permeable stretching sheet was calculated by Chaudhary et al. [12].

The thermal radiation impact on MHD fluid flow via a permeable stretched sheet was examined by Sreenivasulu et al. [13]. Kaladhar et al. [14] explored on the impact of MHD free convective flow across a permeable medium. The movement of electrical current produces heat that is known as the Joule heat phenomenon. Joule heating is often known as Ohmic heating. Joule heating has a regular set of built-up and technological advancement, such as electrical fires, electrical heaters, radiant light bulbs and electrical fuses [15].

When a magnetic field is applied over a stretched sheet, Ghosh [16] estimated the time-dependent flow's characteristics. A significant work on this subject prevail in [17–20]. Because of its importance in aerodynamics and space sciences, suction or injection effects have stimulated the interest of various researchers. Shojaefarde et al. [21] used sunction/injection to regulate the flow on a super sonic aircraft's surface. Makinde and Chinyoka [22] used numerical simulations to study hydromagnetic unsteady flow in a permeable material with in the impact of propulsion parameters. Ganga and Devi [23] investigated the impact of hydrostatic pressure,

viscosity diversion and Joule heating on MHD flow heat conduction through a stretching porous surface immersed in a permeable media.

The tangent hyperbolic fluid demonstration is capable of describing shear rate phenomena. It calculates the amount of fluid required to keep a smaller stream with a higher shear stress rate. The convective heat exchange investigation of non-Newtonian tangent hyperbolic fluid in a certain way by enchanting the impacts of viscous dissipation over a non-linear extending sheet by considering shooting method examined by Hussain et al. [24]. Partha et al. [25] considered the mixed convection stream and heat exchange from an exponentially extending surface in the presence of viscous dissipation.

Mamatha et al. [26] considered the incompressible MHD Carreau Dusty fluid over a extending sheet with exponentially moldering heat source. The concept of viscosity is commonly used in fluid mechanics to characterize the shear properties of a fluid; it can be inadequate to describe non-Newtonian fluids. The properties are way better considered utilizing tensor-valued constitutive conditions, which are common within the field of continuum mechanics. In micropolar fluids, Abel et al. [27] demonstrated how high temperature viscosity affects heat flow over an expanded surface with varying heat conduction. Under the conditions of low Reynolds and long wave length, the unsteady movement of a hyperbolic tangent fluid through a fluid medium in a symmetric porous channel was investigated by Jyothi et al. [28]. Vendabai [29] considered the unsteady boundary layer stream of a nanofluid over a extending surface with variable radiation impact within the rate of heat source. The heat exchange highlights of an unsteady stream of a nanofluid past a extending sheet with a convective boundary condition are deliberate by Mansur and Ishak [30]. The impact of transverse magnetic field and heat source on the boundary layer stream of a Casson nanofluid over a extending exponentially considered by Sarojamma and Vendabai [31].

The tangent hyperbolic fluid model is main model in the non-Newtonian fluids. The tangent hyperbolic fluid is commonly utilised in various laboratory studies. For large-scale magneto-rheological fluid damper coils, Friedman et al. [32] have

used the tangent hyperbolic fluid model. Akbar et al. [33] investigated the influence of magnetohydrodynamics flow heat transmission on tangent hyperbolic fluid across stretched surfaces.

Ibrahim [34] investigated the double stratification's effect on nanofluid boundary-layer flow and heat transfer over a vertical plate. The influence of a magnetic field on the research of nanofluid heat transfer between parallel plates was explained by Hatami et al. [35].

Fakour et al. [36] used the least square approach to investigate the heat and mass transport features of squeezing a micropolar fluid within a porous media. Haile and Shankar [37] studied the impacts of thermal radiation, thick scattering, and chemical reaction on heat and mass exchange of MHD stream of nanofluids through a permeable medium. They observed that as the thermal radiation or thick scattering increases, it causes increase in temperature of the coolant liquid.

Uddin et al. [38] analyzed the free convection stream of magnetic nanofluid with chemical reaction detected that as the stream speed is decreased by the magnetic field, the temperature of the liquid increases. The chemical reaction can further intimate heterogeneous and homogenous processes.

In the case of rugged compound system, the reaction is heterogenous. Magyari and Chamkha et al. [39] studied the impact of chemical reaction and radiation on MHD nanofluid flow in permeable medium by using the method of spectral relaxation. They observed that velocity profile decreases with increase in porosity parameter.

Chamkha and Rashad [40] debated the effect of chemical reaction on MHD flow in the existence of heat generation or assimilation of uniform perpendicular absorptive surface. Das [41] delineated the consequences of chemical reaction with radiation on the heat and mass swapping along the MHD flow. Graphs and tables are used to explain the physical behaviour of the useful parameters. Numerically, the coefficient of skin friction, the local Nusselt number and local Sherwood number are computed.

1.1 Thesis Contributions

In this thesis, a review study of Ibrahim [42] has been presented and then extended for the tangent hyperbolic fluid and chemical reaction. The problem is modeled as nonlinear PDEs which are converted into a system of ODEs by using appropriate transformation of similarities. Numerical results are obtained by using the shooting technique with Runge-Kutta method of order four (RK4) in MATLAB. The influence of various relevant physical parameters such as magnetic field parameter M, suction and injection parameter S, Eckert number Ec, Prandtl number Pr, radiation parameter R, heat generation parameter Q, permeability parameter λ, Weizenberg number We, chemical reaction parameter r and Schmidt number Sc on the velocity profile $f'(\xi)$, temperature profile $\theta(\xi)$, concentration profile $\phi(\xi)$, skin friction coefficient C_f, local Nusselt number Nu_x and Sherwood number Sh_x are analyzed graphically as well as in tabular form.

1.2 Dissertation Outline

This research work is further divided into four key chapters.

Chapter 2 demonstrates some important definitions and basic laws that are usefull in understanding the work in upcoming chapters.

Chapter 3 describes the numerical investigation of impact of radiative MHD flow with Joule heating over a stretching porous sheet. This chapter is the review of Ibrahim et al. [42].

Chapter 4 presents the model given in [42] by considering the additional impact of tangent hyperbolic fluid model and chemical reaction. The dimensionless ODEs are solved mathematically by method of shooting. Effect of different physical parameters are illustrated using tables and graphs.

Chapter 5 recapitulate the thesis work and gives the major results obtained from the entire research and suggests recommendations for the future work.

All the references used in this research work are listed in ***Bibliography***.

Chapter 2

Basic Concepts and Governing Equations

Some definitions, basic laws and terminologies are presented in the current chapter, which will be used in the next chapters.

2.1 Important Definitions

Definition 2.1.1 (Fluid)

"A fluid is a substance that deforms continuously under the application of a shear stress no matter how small the shear stress may be" [43].

Definition 2.1.2 (Fluid Mechanics)

"Fluid mechanics is defined as the science that deals with the behavior of fluids at rest (fluid statics) or in motion (fluid dynamics) and the interaction of fluids with solid or other fluids at the boundaries" [43].

Definition 2.1.3 (Fluid Statics)

"The study of fluid at rest is called fluid statics" [44].

Definition 2.1.4 (Fluid Dynamics)

"The study of fluids in motion if the pressure forces are also considered is called fluid dynamics" [44].

Definition 2.1.5 (Fluid Kinematics)

"The study of fluids in motion, where pressure forces are not considered, is called fluid kinematics"[44].

Definition 2.1.6 (Viscosity)

"Viscosity is defined as the property of a fluid which offers resistance to the movement of one layer of fluid over another adjacent layer of the fluid. Mathematically,

$$\mu = \frac{\tau}{\frac{\partial u}{\partial y}}$$

where μ is viscosity coefficient, τ is shear stress

and $\frac{\partial u}{\partial y}$ represents the velocity gradient"[44].

Definition 2.1.7 (Magnetohydrodynamics)

"Magnetohydrodynamics (MHD) is concerned with the flow of electrically conducting fluids in the presence of magnetic fields, either externally applied or generated within the fluid by inductive action" [45].

Definition 2.1.8 (Nanofluids)

"Nanofluids are engineered by suspending nanoparticles with average sizes below 100 nm in traditional heat transfer fluids such as water, oil, and ethylene glycol.

A very small amount of guest nanoparticles, when dispersed uniformly and suspended stably in host fluids, can provide dramatic improvements in the thermal properties of host fluids" [46].

Definition 2.1.9 (Density)

"Density is defined as mass per unit volume.

That is $\mu = \frac{m}{v}$, where, v is the volume" [43] .

Definition 2.1.10 (Pressure)

"Pressure is defined as a normal force exerted by a fluid per unit area. We speak of pressure only when we deal with a gas or a liquid.

It is formulated as: $p = \frac{F}{A}$" [43].

Definition 2.1.11 (Boundary Layer)

"The region where viscous effects are dominant are known as boundary layer region around which fluid is flowing. The concept of boundary layer, implies that flow at high Reynold numbers can be divided into two unequally large regions. In the bulk of flow region, the viscosity can be neglected, and the flow corresponds to the inviscid limiting solution. This is called the inviscid outer flow.

The second region is the very thin boundary layer at wall where the viscosity must be taken into account. Within the boundary layer the two different flow forms, that is, the flow can be laminar or turbulent " [47].

2.2 Types of Flow

Definition 2.2.1 (Steady vs Unsteady Flow)

" The term steady implies no change of properties, velocity, temperature, etc., at a point with time. The opposite of steady is unsteady" [43].

Definition 2.2.2 (Laminar vs Turbulent Flow)

"Some flows are smooth and orderly while others are rather chaotic. The highly ordered fluid motion characterized by smooth layers of fluid is called laminar.

The highly disordered fluid motion that typically occurs at high velocities and is characterized by velocity fluctuations is called turbulent" [43].

Definition 2.2.3 (Uniform Flow)

"The simplest plane flow is one for which the streamlines are all straight and parallel, and the magnitude of the velocity is constant. This type of flow is called a uniform flow" [48].

Definition 2.2.4 (Natural vs Forced Flow)

"A fluid flow is said to be natural or forced, depending on how the fluid motion is initiated. In forced flow, a fluid is forced to flow over a surface or in a pipe by external means. Whereas In natural flows, fluid motion is due to natural means such as the buoyancy effect" [43].

Definition 2.2.5 (External vs Internal Flow)

"The flow of an unbounded fluid over a surface such as a plate, a wire, or a pipe is external flow.

The flow in a pipe or duct is internal flow if the fluid is completely bounded by solid surfaces. For example, flow of water in a pipe is internal flow" [49].

Definition 2.2.6 (Viscous vs Inviscous Flow)

"When two fluid layers move relative to each other, a friction force develops between them and the slower layer tries to slow down the faster layer. This internal resistance to flow is quantified by the fluid property viscosity, which is a measure of internal stickiness of the fluid.

Viscosity is caused by cohesive forces between the molecules in liquids and by molecular collisions in gases. There is no fluid with zero viscosity, and thus all fluid flows involve viscous effects to some degree.

Flows in which the frictional effects are significant are called viscous flows. However, in many flows of practical interest, there are regions (typically regions not close to solid surfaces) where viscous forces are negligibly small compared to inertial or pressure forces. Neglecting the viscous terms in such inviscid flow regions greatly simplifies the analysis without much loss in accuracy" [43].

2.3 Classifications and Properties of Fluid

Definition 2.3.1 (Compressible vs Incompressible Flow)

"A flow is classified as being compressible or incompressible, depending on the level of variation of density during flow.

Incompressibility is an approximation, and a flow is said to be incompressible if the density remains nearly constant throughout. Therefore, the volume of every portion of fluid remains unchanged over the course of its motion when the flow (or the fluid) is incompressible.

The densities of liquids are essentially constant, and thus the flow of liquids is typically incompressible. Therefore, liquids are usually referred to as incompressible substances.

A pressure of 210 atm, for example, causes the density of liquid water at 1 atm to change by just 1 percent. Gases, on the other hand, are highly compressible.

A pressure change of just 0.01 atm, for example, causes a change of 1 percent in the density of atmospheric air" [43].

Definition 2.3.2 (Newtonian Fluids vs non-Newtonian Fluids)

"Fluids for which the rate of deformation is linearly proportional to the shear stress are called Newtonian fluids.

In one-dimensional shear flow of Newtonian fuids, shear stress can be expressed by the linear relationship as

$$\tau_{yx} = \mu \left(\frac{\partial u}{\partial y} \right)^n, \tag{2.1}$$

where the constant of proportionality μ is called the coefficient of viscosity or the dynamic (or absolute) viscosity of the fluid." Examples are air, water, kerosene and gasoline. "Fluids for which the shear stress is not linearly related to the shear strain rate are called non-Newtonian fluids" [43].

Definition 2.3.3 (Ideal vs Real Fluid)

"An ideal fluid is defined as a non-viscous and incompressible fluid. That is the fluid has zero viscosity and a constant density ($\rho = constant, \mu = 0$).

Although no ideal fluid exists, many real fluid have small viscosity and the effects of compressibility are negligible" [50].

2.4 Heat Transfer Mechanism and related Properties

Definition 2.4.1 (Conduction)

"Conduction is the transfer of heat from one part of a body at a higher temperature to another part of the same body at a lower temperature" [51].

Definition 2.4.2 (Convection)

"Convection, relates to the transfer of heat from a bounding surface to a fluid in motion, or to the heat transfer across a ow plane within the interior of the flowing fluid" [51].

Definition 2.4.3 (Forced Convection)

"If the fluid motion is induced by a pump, a blower, a fan, or some similar device, the process is called forced convection" [51].

Definition 2.4.4 (Natural Convection)

"If the fluid motion occurs as a result of the density difference produced by the temperature difference, the process is called free or natural convection." [51]

Definition 2.4.5 (Mixed Convection)

"Mixed convection occurs when both natural convection and forced convection play significant roles in the transfer of heat. Mixed convection occurs when the heat transfer is significantly different from that for pure natural convection " [51].

Definition 2.4.6 (Radiation)

"Radiation, or more correctly thermal radiation, is electromagnetic radiation emitted by a body by virtue of its temperature and at the expense of its internal energy. All heated solids and liquids, as well as some gases, emit thermal radiation. The transfer of energy by conduction requires the presence of a material medium, while radiation does not" [51].

Definition 2.4.7 (Thermal Conductivity)

"The Fourier heat conduction law states that the heat flow is proportional to the temperature gradient. The coefficient of proportionality is a material parameter known as the thermal conductivity which may be a function of a number of variables" [52].

Definition 2.4.8 (Thermal Diffusivity)

"The rate at which heat diffuses by conducting through a material depends on the thermal diffusivity and can be defined as:

$$\alpha = \frac{\kappa}{\rho C_p},$$

where α is the thermal diffusivity, κ is the thermal conductivity, ρ is the density and C_p is the specific heat at constant pressure" [52].

2.5 Fundamental Equations and Conservation Laws

2.5.1 Continuity Equation

"The conservation of mass of fluid entering and leaving the control volume, the resulting mass balance is called the equation of continuity. This equation reflects the fact that mass is conserved. Mathematically, it can be written as

$$\frac{\partial \rho}{\partial t} + \nabla.(\rho \mathbf{V}) = 0.$$

For steady case rate of time will be constant, so continuity equation becomes

$$\nabla.\left(\rho \mathbf{V}\right) = 0.$$

In the case of incompressible flow, density does not variate so continuity equation can be written as, $\nabla.\left(\mathbf{V}\right) = 0$,

where, $\mathbf{V}$ is the velocity of fluid" [53].

2.5.2 Momentum Equation

"For any fluid the momentum equation is

$$\frac{\partial}{\partial t}\left(\rho \mathbf{V}\right) + \nabla.[\left(\rho \mathbf{V}\right)\mathbf{V}] - \nabla.\mathbf{T} - \rho \mathbf{g} = 0, \tag{2.2}$$

since $\mathbf{T} = -pI + \tau$, the momentum equation takes the form

$$\rho\left(\frac{\partial \mathbf{V}}{\partial t} + \mathbf{V}.\nabla \mathbf{V}\right) = \nabla.\left(-pI + \tau\right) + \rho \mathbf{g}. \tag{2.3}$$

Equation (2.2) is a vector equation and can be decomposed further into three scaler components by taking the scaler product with the basis vectors of an appropriate orthogonal coordinate system.

By setting $\mathbf{g} = g\nabla z$, where z is the distance from an arbitrary reference elevation in the direction of gravity, Eq. (2.2) can also be expressed as

$$\rho\frac{D\mathbf{V}}{Dt} = \rho\left(\frac{\partial \mathbf{V}}{\partial t} + \mathbf{V}.\nabla \mathbf{V}\right) = \nabla.\left(-pI + \tau\right) + \rho(g\nabla z), \tag{2.4}$$

where $\frac{D}{Dt}$ is the substantial derivative.

The momentum equation then states that the acceleration of a particle following the motion is the result of net force, expressed by the gradient of pressure, viscous and gravity forces" [53].

2.5.3 Energy Equation

"Conservation of thermal energy is expressed by

$$\rho \left[\frac{\partial U}{\partial t} + \mathbf{V}.\nabla U \right] = \tau : \nabla \mathbf{V} + p\nabla.\mathbf{V}\nabla \left(k\nabla T \right) \pm H_r, \qquad (2.5)$$

By involving the definition of the internal energy ,

$$\rho C_v \left[\frac{\partial T}{\partial t} + \mathbf{V}.\nabla T \right] = \tau : \nabla \mathbf{V} + p\nabla.\mathbf{V}\nabla \left(k\nabla T \right) \pm H_r. \qquad (2.6)$$

For heat conduction in solid i.e. when $\mathbf{V} = 0, \nabla \mathbf{V} = 0$ and $C_v = C$ the resulting equation is

$$\rho C \frac{\partial T}{\partial t} = \nabla \left(k\nabla T \right) \pm H_r. \qquad (2.7)$$

Where U is the internal energy per unit mass, and H_r is the heat of reaction" [53].

2.6 Solution Methodology

To elaborate the shooting method, consider the following nonlinear boundary value problem.

$$\left. \begin{array}{ll} f''(x) = f(x)f'(x) + 2f^2(x) \\ f(0) = 0 \qquad\qquad f(G) = L \end{array} \right\} \qquad (2.8)$$

Introduce the following notations, to reduce the order of the above boundary value problem.

$$f = E_1, \qquad f' = E_1' = E_2, \qquad f'' = E_2'. \qquad (2.9)$$

As a result, (2.8) is converted into the following system of first order ODEs.

$$E_1' = E_2, \qquad\qquad E_1(0) = 0, \qquad (2.10)$$

$$E_2' = E_1 E_2 + 2E_1^2, \qquad\qquad E_2(0) = w, \qquad (2.11)$$

where w denotes the missing initial condition that will be guessed.

The RK4 method will be used to solve the above IVP numerically. The missing condition w must be selected in such a way that.

$$E_1(G, w) = L. \qquad (2.12)$$

For convenience, now onward $E_1(G, w)$ will be denoted by $E_1(w)$.

Let us further denote $E_1(w) - L = X(w)$, so that

$$X(w) = 0. \qquad (2.13)$$

The following iterative formula can be used to solve the given equation using Newton's method.

$$w^{n+1} = w^n - \frac{X(w^n)}{\frac{\partial X(w^n)}{\partial w}}, \quad n = 0, 1, 2, 3, \ldots. \qquad (2.14)$$

or

$$w^{n+1} = w^n - \frac{E_1(w^n) - L}{\frac{\partial E_1(w^n)}{\partial w}}. \qquad (2.15)$$

For solving (2.15), introduce the following notations.

$$\frac{\partial E_1}{\partial w} = E_3, \quad \frac{\partial E_2}{\partial w} = E_4. \tag{2.16}$$

Using these new notations the Newton's iterative scheme, will then get the form.

$$w^{n+1} = w^n - \frac{E_1(w^n) - L}{E_3(w^n)}. \tag{2.17}$$

Now differentiating the system of two first order ODEs (2.10)-(2.11) with respect to w, we get another form of ODEs, as follows.

$$E_3' = E_4, \qquad\qquad E_3(0) = 0. \tag{2.18}$$

$$E_4' = E_3 E_2 + E_1 E_4 + 4 E_1 E_3, \qquad\qquad E_4(0) = 1. \tag{2.19}$$

We have the following initial value problem when we combine the four ODEs (2.10), (2.11), (2.18) and (2.19).

$$E_1' = E_2, \qquad\qquad E_1(0) = 0,$$

$$E_2' = E_1 E_2 + 2 E_1^2, \qquad\qquad E_2(0) = w,$$

$$E_3' = E_4, \qquad\qquad E_3(0) = 0.$$

$$E_4' = E_3 E_2 + E_1 E_4 + 4 E_1 E_3, \qquad\qquad E_4(0) = 1.$$

The above system will be solved numerically by Runge-Kutta method of order four.

The stopping criteria for the Newton's technique is set as,

$$|E_1(w) - L| < \epsilon,$$

where $\epsilon > 0$ is an arbitrarily small positive number.

2.7 Dimensionless Parameters

Definition 2.6.1 (Nusselt Number Nu_x)

"It is the ratio of the convective to the conductive heat transfer at a boundary in a fluid. Mathematically,

$$Nu_x = \frac{hL}{k},$$

where h stands for convective heat transfer, L for the characteristics length and k stands for the thermal conductivity" [54].

Definition 2.6.2 (Skin Friction Coefficient C_{fx})

"Skin friction coefficient occurs between the fluid and the solid surface which leads to slow down the motion of the fluid. The skin friction coefficient can be defined as

$$C_{fx} = \frac{2\tau_w}{\rho U^2},$$

where τ_w denotes the wall shear stress, ρ the density and U the free-stream velocity" [54].

Definition 2.6.3 (Sherwood Number)

"It expresses the ratio of the heat transfer to the molecular diffusion. It characterizes the mass transfer intensity at the interface of phases" [55].

Definition 2.6.4 Prandtl Number (Pr)

"It is the ratio between the momentum diffusivity (ν) and thermal diffusivity (α). Mathematically, it can be defined as

$$Pr = \frac{\nu}{\alpha} = \frac{\mu/\rho}{k/c_p} = \frac{\mu C_p}{k},$$

where μ represents the dynamic viscosity, C_p denotes the specific heat and k stands for thermal conductivity.

The relative thickness of thermal and momentum boundary layer is controlled

by Prandtl number. For small Pr, heat distributed rapidly corresponds to the momentum" [54].

Definition 2.6.5 Eckert Number (Ec)

"It is the dimensionless number used in continuum mechanics. It describes the relation between flows and the boundary layer enthalpy difference and it is used for characterized heat dissipation" [54].

Definition 2.6.6 (Schmidt Number)

"This number expresses the ratio of the kinematic viscosity, or momentum transfer by internal friction, to the molecular diffusivity. It characterizes the relation between the material and momentum transfers in mass transfer" [55].

Definition 2.6.7 (Reynolds Number)

"It is defined as the ratio of inertia force of a flowing fluid and the viscous force of the fluid. Mathematically,

$$Re_x = \frac{VL}{\nu}$$

where V denotes the free stream velocity, L is the characteristic length and ν stands for kinematic viscosity"[44].

Definition 2.6.8 (Weissenberg Number We)

"The dimensionless Weissenberg number, formulated by German physicist Karl Weissenberg, is defined as

$$We = \frac{\rho \mathbf{U}^2}{\tau}, \tag{2.20}$$

where ρ is the fluid density, $\mathbf{U}$ denotes the flow velocity and τ stands for the shear stress.

This number expresses the characteristic material time (relaxation time) and the shear velocity. It characterizes the velocity and time relations in rheological processes in viscoelastic shear flow. Furthermore, it also expresses the ratio of the dynamic viscoelastic force to the viscous force" [55].

Chapter 3

Radiative MHD Flow with Joule Heating over a Stretched Porous Sheet

3.1 Introduction

In this chapter, an exploration on MHD flow over a porous stretching sheet in the presence of magnetic field, heat generation and heat source. By using similarity variables, the governing non-linear PDEs are converted into ODEs. By using shooting technique, the solution of ordinary differential equation is obtained. At the end of this chapter, the impact of various parameters of the transformed ODEs is discussed for dimensionless velocity, temperature, Nusselt number and skin friction coefficient. Investigation of numerical results is presented through graph and tables. This chapter provides a detailed review of Ibrahim et al. [42].

3.2 Mathematical Modeling

In the existence of viscous dissipation and heat conduction, we investigate a steady, radiative flow of a viscous liquid in 2D over a permeable stretching sheet arranged

at $y = 0$. The direction of the flow is taken along x-axis while y-axis is considered normal to it. In the perpendicular direction to the sheet, a uniform magnetic field of strength B_0 is applied. The sheet's stretching velocity is considered to be $u_w = cx$, where c is a positive constant. Figure 3.1 depicts the flow configuration and coordinate system. Along the x-axis two equal and opposite forces are applied to stretch the surface while maintaining the origin stationary.
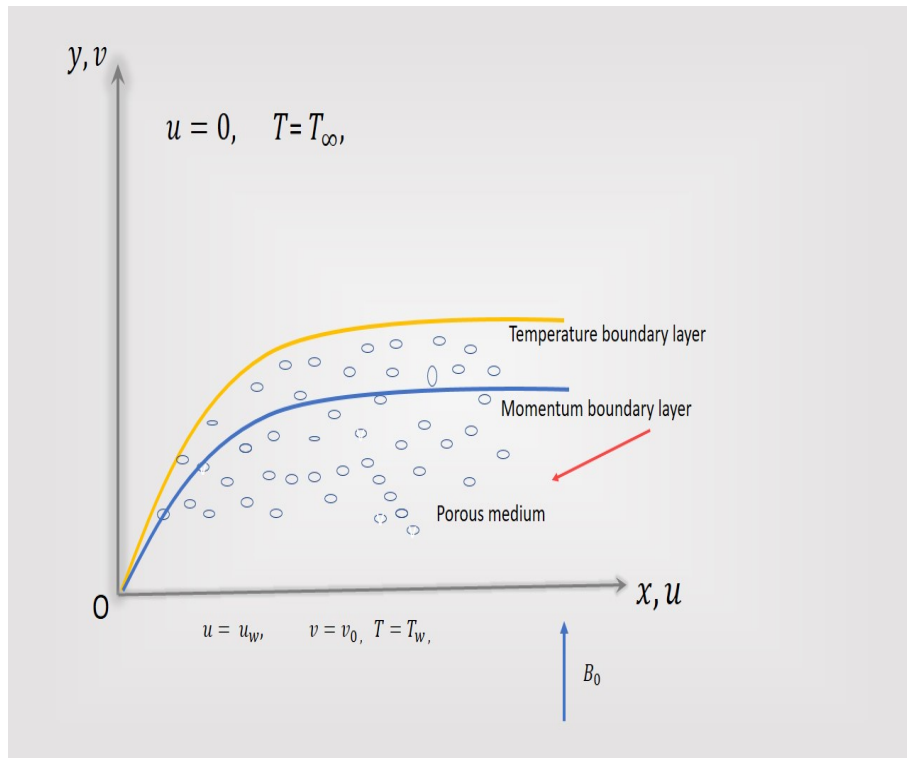

FIGURE 3.1: Physical configuration

3.3 The Governing Equations

The flow is explained by considering the $2D$ governing equations containing the continuity, momentum and energy as follow:

- Continuity Equation:

$$\frac{\partial u}{\partial x} + \frac{\partial v}{\partial y} = 0, \tag{3.1}$$

- Momentum Equation:

$$u\frac{\partial u}{\partial x} + v\frac{\partial u}{\partial y} = \nu\frac{\partial^2 u}{\partial y^2} - \frac{\sigma B_0^2}{\rho}u - \frac{\nu}{K_p}u, \tag{3.2}$$

- Energy Equation:

$$u\frac{\partial T}{\partial x} + v\frac{\partial T}{\partial y} = \frac{k}{\rho C_p}\frac{\partial^2 T}{\partial y^2} + \frac{\nu}{C_p}\left(\frac{\partial u}{\partial y}\right)^2 - \frac{1}{\rho C_p}\frac{\partial q_r}{\partial y} + \frac{\sigma B_0^2}{\rho C_p}u^2 + \frac{Q_0}{\rho C_p}(T_\infty - T). \tag{3.3}$$

Boundary Conditions The dimensional form of the boundary conditions is given as.

$$\left.\begin{aligned} u = cx, \quad v = -v_0, \quad \frac{\partial T}{\partial y} = Bx^2, \qquad \text{at} \quad y = 0, \\ u = 0, \quad T = T_\infty, \quad \text{as} \qquad y \to \infty. \end{aligned}\right\} \tag{3.4}$$

In the preceding model, u and v are velocity components in x and y directions, respectively. The x and y are axial and normal coordinates. T is a fluid temperature, B_0 is magnetic field strength, σ is the electrical conductivity, ν is the kinematic viscosity, ρ is the density of the fluid, k is thermal conductivity, C_p is the specific heat at constant pressure and K_p is the permeability of porous medium.In 1904, Ludwig Prandtl first define the aerodynamic boundary layer at the third International Congress of Mathematician in Heidleberg Germany. After that one of his student Henry Blasius presented the boundary layer approximation with similarity transformation. By boundary layer approximation theory, here we have considered those terms which have greater impact of magnitude while eliminated those who have less impact of magnitude from the well known Navier-Stokes equations. Here q_r known as Rosseland radiative heat flux which can be defined as

$$q_r = -\frac{4\sigma^*}{3k^*}\frac{\partial T^4}{\partial y}, \tag{3.5}$$

where k^*(absorption coefficient) and σ^* (Boltzman constant). By applying Taylor series, T^4 can be expanded about T_∞ which is ambient temperature.

$$T^4 = T_\infty^4 + 4T_\infty^3(T - T_\infty) + \frac{12T_\infty^2}{2!}(T - T_\infty)^2 + \frac{24T_\infty}{3!}(T - T_\infty)^3 + ...$$

By ignoring the higher order terms of the reduced Taylor series gets the form

$$T^4 = T_\infty^4 + 4T_\infty^3(T - T_\infty).$$

thus, we have

$$\frac{\partial T^4}{\partial y} = 4T^3 \frac{\partial T}{\partial y}. \tag{3.6}$$

Using Eq. (3.6) in Eq. (3.5) and differentiate Eq. (3.5) with respect to y,

$$\frac{\partial q_r}{\partial y} = -\frac{16\sigma^* T_\infty^3}{3k^*} \frac{\partial^2 T}{\partial y^2}. \tag{3.7}$$

$$\left.\begin{array}{l} u = cxf'(\xi), \quad v = -\sqrt{c\nu}f(\xi), \\[2mm] \xi = y\sqrt{\dfrac{c}{\nu}}, \quad T = T_\infty + Bx^2\sqrt{\dfrac{\nu}{c}}\theta(\xi). \end{array}\right\} \tag{3.8}$$

The detailed procedure for conversion the Eqs. (3.1)-(3.3) into non-dimensional form has been described as follows. First, we include the below procedure for the conversion of Eq. (3.1) into the dimensionless form. So in order to derive the left hand side of the Eq. (3.1) following procedure is adopted.

$$u = cxf'(\xi). \tag{3.9}$$

$$v = -\sqrt{c\nu}f(\xi). \tag{3.10}$$

Differentiate Eq. (3.9) w.r.t. 'x'

$$\frac{\partial u}{\partial x} = \frac{\partial}{\partial x}\left(cxf'(\xi)\right),$$
$$\frac{\partial u}{\partial x} = cf'(\xi). \tag{3.11}$$

Similarly, differentiating Eq. (3.10) w.r.t. 'y'

$$\frac{\partial v}{\partial y} = \frac{\partial}{\partial y}\left(-\sqrt{c\nu}f(\xi)\right),$$

$$\frac{\partial v}{\partial y} = -f'(\xi)\sqrt{c\nu}\sqrt{\frac{c}{\nu}},$$

$$\frac{\partial v}{\partial y} = -cf'(\xi). \tag{3.12}$$

Adding Eq. (3.11) and (3.12), we get (3.1),

$$\frac{\partial u}{\partial x} + \frac{\partial v}{\partial y} = cf'(\xi) - cf'(\xi),$$

$$\frac{\partial u}{\partial x} + \frac{\partial v}{\partial y} = 0. \tag{3.13}$$

Hence the continuity equation is satisfied, identically. Now we include the procedure for the conversion of Eq. (3.2) into dimensionless form, So in order to derive the left hand side of the Eq. (3.2) following procedure is adopted.

$$u\frac{\partial u}{\partial x} + v\frac{\partial u}{\partial y} = cxf'(\xi)\frac{\partial}{\partial x}(cxf'(\xi)) + (-\sqrt{c\nu}f(\xi)\frac{\partial}{\partial y}(cxf'(\xi),$$

$$u\frac{\partial u}{\partial x} + v\frac{\partial u}{\partial y} = cxf'(\xi)cf'(\xi) + (-\sqrt{c\nu}f(\xi)\frac{1}{\sqrt{\nu}}c^{\frac{3}{2}}xf''(\xi)),$$

$$u\frac{\partial u}{\partial x} + v\frac{\partial u}{\partial y} = c^2xf'^2(\xi) - c^2xff''. \tag{3.14}$$

Similarly for the derivation of right hand side of Eq. (3.2) following steps will be useful.

$$\nu\frac{\partial^2 u}{\partial y^2} - \frac{\sigma B_0^2}{\rho}u - \frac{\nu}{K_p}. \tag{3.15}$$

Differentiating Eq. (3.9) w.r.t. 'y'

$$\frac{\partial u}{\partial y} = \frac{\partial}{\partial y}cxf'(\xi),$$

$$\frac{\partial u}{\partial y} = \frac{c^{\frac{3}{2}}}{\nu}xf''(\xi).$$

Again differentiating above relation w.r.t. 'y''

$$\frac{\partial^2 u}{\partial y^2} = \frac{c^{\frac{3}{2}}}{\nu} x f'''(\xi) \sqrt{\frac{c}{\nu}},$$

$$\frac{\partial^2 u}{\partial y^2} = \frac{c^2 x}{\nu} f'''(\xi). \tag{3.16}$$

By putting Eq. (3.16) in Eq. (3.15)

$$= c^2 x f'''(\xi) - \frac{\sigma B_0^2}{\rho} \rho c x f'(\xi) - \frac{\nu}{K_p} c x f'(\xi),$$

$$= c^2 x f'''(\xi) - \left(\frac{\sigma B_0^2}{\rho} + \frac{\nu}{K_p}\right) c x f'(\xi). \tag{3.17}$$

Now Combining Eqs. (3.14) and Eq. (3.17)

$$c^2 x f'^2(\xi) - c^2 x f f'' = c^2 x f'''(\xi) - \left(\frac{\sigma B_0^2}{\rho} + \frac{\nu}{K_p}\right) c x f'(\xi),$$

$$c^2 x f'''(\xi) - \left(\frac{\sigma B_0^2}{\rho} + \frac{\nu}{K_p}\right) c x f'(\xi) - c^2 x f'^2(\xi) + c^2 x f f'' = 0.$$

Dividing by '$c^2 x$'

$$f''' + f f'' - f'^2 - (M + \lambda) f' = 0.$$

Where $M = \frac{\sigma B_0^2}{\rho c}$, $\quad \lambda = \frac{\nu}{K_p c}$, are magnetic and porosity parameter respectively.

Next converting the energy equation into the dimensionless form.

By using the Eq. (3.8) into Eq. (3.3)

$$T = T_\infty + B x^2 \sqrt{\frac{\nu}{c}} \theta(\xi). \tag{3.18}$$

Differentiating Eq. (3.18) w.r.t 'x'' we have

$$\frac{\partial T}{\partial x} = \frac{\partial}{\partial x} \left(B x^2 \sqrt{\frac{\nu}{c}} \theta(\xi)\right),$$

$$\frac{\partial T}{\partial x} = 2 B x \sqrt{\frac{\nu}{c}} \theta(\xi). \tag{3.19}$$

Similarly, differentiating Eq. (3.18) w.r.t 'y''

$$\frac{\partial T}{\partial y} = Bx^2\sqrt{\frac{\nu}{c}}\theta'(\xi)\sqrt{\frac{c}{\nu}},$$

$$\frac{\partial T}{\partial y} = Bx^2\theta'(\xi). \tag{3.20}$$

Now using Eqs. (3.19) and (3.20) into the left hand side of Eq. (3.3)

$$= u\frac{\partial T}{\partial x} + v\frac{\partial T}{\partial y},$$

$$= cxf'(\xi)2Bx\sqrt{\frac{\nu}{c}}\theta(\xi) - \left(\sqrt{c\nu}f(\xi)Bx^2\theta'(\xi)\right),$$

$$= \sqrt{c\nu}f'(\xi)2Bx^2\theta(\xi) - \sqrt{c\nu}f(\xi)Bx^2\theta'(\xi). \tag{3.21}$$

Now using Eq. (3.8) into the right hand side of Eq. (3.3), we have

$$= \frac{k}{\rho C_p}\frac{\partial^2 T}{\partial y^2} + \frac{\nu}{C_p}\left(\frac{\partial u}{\partial y}\right)^2 - \frac{1}{\rho C_p}\frac{\partial q_r}{\partial y} + \frac{\sigma B_0^2}{\rho C_P}u^2 + \frac{Q_0}{\rho C_p}(T_\infty - T),$$

$$= \frac{k}{\rho C_p}\frac{\partial^2}{\partial y^2}\left(T_\infty + Bx^2\sqrt{\frac{\nu}{c}}\theta(\xi)\right) + \frac{\nu}{C_p}\left(\frac{\partial}{\partial y}\left(cxf'(\xi)\right)\right)^2 - \frac{1}{\rho C_p}\frac{\partial}{\partial y}\left(\frac{-4\sigma^*}{3k^*}\frac{\partial T^4}{\partial y}\right)$$

$$+ \frac{\sigma B_0^2}{\rho C_p}\left(cxf'(\xi)\right)^2 + \frac{Q_0}{\rho C_p}\left(T_\infty - T_\infty - Bx^2\sqrt{\frac{\nu}{c}}\theta(\xi)\right),$$

$$= \frac{k}{\rho C_p}\frac{\partial}{\partial y}\left(Bx^2\sqrt{\frac{\nu}{c}}\theta'(\xi)\sqrt{\frac{c}{\nu}}\right) + \frac{\nu}{C_p}c^2x^2\left(f''(\xi)\right)^2\frac{c}{\nu} + \frac{1}{\rho C_p}\frac{16}{3}\frac{\sigma^*T^3}{k^*}\frac{\partial^2 T}{\partial y^2}$$

$$+ \frac{\sigma B_0^2}{\rho C_p}c^2x^2f'^2(\xi) + \frac{Q_0}{\rho C_p}\left(-Bx^2\sqrt{\frac{\nu}{c}}\theta(\xi)\right),$$

$$= \frac{k}{\rho C_p}\left(\theta''(\xi)Bx^2\sqrt{\frac{c}{\nu}}\right) + \frac{1}{C_p}(c^3x^2)f''^2(\xi) + \frac{1}{\rho C_p}\frac{16}{3}\frac{\sigma^*T^3}{k^*}\theta''(\xi)Bx^2\sqrt{\frac{c}{\nu}}$$

$$+ \frac{\sigma B_0^2}{\rho C_p}c^2x^2f'^2(\xi) + \frac{Q_0}{\rho C_p}\left(-Bx^2\sqrt{\frac{\nu}{c}}\theta(\xi)\right),$$

$$= \frac{k}{\rho C_p}\left(\theta''(\xi)Bx^2\sqrt{\frac{c}{\nu}}\right) + \frac{16\sigma^*T_\infty^3}{\rho C_p 3k^*}\left(\theta''(\xi)Bx^2\sqrt{\frac{c}{\nu}}\right)$$

$$+ \frac{\sigma B_0^2}{\rho C_p}c^2x^2f'^2(\xi) + \frac{Q_0}{\rho C_p}\left(-Bx^2\sqrt{\frac{\nu}{c}}\theta(\xi)\right) + \frac{1}{C_p}\left(c^3x^2f''^2(\xi)\right). \tag{3.22}$$

Multiplying Eq. (3.21) by $\frac{\rho C_P}{kBx^2}\sqrt{\frac{\nu}{c}}$

$$\frac{\rho C_p}{kBx^2}\sqrt{\frac{\nu}{c}}\left(\sqrt{c\nu}f'(\xi)2Bx^2\theta(\xi)\right) - \frac{\rho C_p}{kBx^2}\sqrt{\frac{\nu}{c}}\left(\sqrt{c\nu}f'(\xi)2Bx^2\theta(\xi)\right),$$

$$\Rightarrow \quad \frac{\rho C_p}{kBx^2}\nu f'(\xi)\theta(\xi)2Bx^2 - \frac{\nu\rho C_p}{k}\theta'(\xi)f(\xi),$$

(3.23)

$$\Rightarrow \quad 2Prf'(\xi)\theta(\xi) - Pr\theta'(\xi)f(\xi).$$

(3.24)

Multiplying Eq. (3.22) by $\frac{\rho C_p}{kBx^2}\sqrt{\frac{\nu}{c}}$

$$\Rightarrow \quad \frac{\rho C_p}{kBx^2}\sqrt{\frac{\nu}{c}}\left(\frac{k}{\rho C_p}(\theta''(\xi)Bx^2\sqrt{\frac{c}{\nu}})\right) + \frac{\rho C_p}{kBx^2}\sqrt{\frac{\nu}{c}}\left(\frac{c^3x^2}{C_p}f''^2(\xi)\right)$$

$$+ \frac{\rho C_p}{kBx^2}\sqrt{\frac{\nu}{c}}\left(\frac{\sigma B_0^2}{\rho C_p}c^2x^2f'^2(\xi)\right) - \frac{\rho C_p}{kBx^2}\sqrt{\frac{\nu}{c}}\frac{Q_0}{\rho C_p}\left(Bx^2\sqrt{\frac{\nu}{c}}\theta(\xi)\right)$$

$$+ \frac{\rho C_p}{kBx^2}\sqrt{\frac{\nu}{c}}\left(\frac{16\sigma^*T_\infty^3}{\rho C_P 3k^*}(\theta''(\xi))Bx^2\sqrt{\frac{c}{\nu}}\right),$$

$$\Rightarrow \quad \theta''\left(1+\frac{4}{3}R\right) + \frac{c^3\rho C_p}{kBC_p}\sqrt{\frac{\nu}{c}}f''^2(\xi) + \frac{\rho C_p\sigma B_0^2c^2}{kB\rho C_p}\sqrt{\frac{\nu}{c}}f'^2(\xi) - PrQ\theta.$$

Multiplying and dividing by '$c\nu$'

$$\theta''\left(1+\frac{4}{3}R\right)\frac{c\nu}{c\nu} + \frac{c^3\rho C_p}{kBC_p}\sqrt{\frac{\nu}{c}}f''^2(\xi)\frac{c\nu}{c\nu} + \frac{\rho C_p\sigma B_0^2c^2}{kB\rho C_p}\sqrt{\frac{\nu}{c}}\frac{c\nu}{c\nu}f'^2(\xi) - \frac{c\nu}{c\nu}PrQ\theta,$$

$$\theta''(1+\frac{4}{3}R) + PrEc\left(f''^2 + Mf'^2\right) - PrQ\theta.$$

(3.25)

Combining Eq. (3.24) and (3.25)

$$2Prf'(\xi)\theta(\xi) - Pr\theta'(\xi)f(\xi) = \theta''(1+\frac{4}{3}R) + PrEc\left(f''^2 + Mf'^2\right) - PrQ\theta,$$

$$(1+\frac{4}{3}R)\theta'' + Pr\theta'(\xi)f(\xi) - 2Prf'(\xi)\theta(\xi) + PrEc\left(f''^2 + Mf'^2\right) - PrQ\theta = 0.$$

Next for converting the associated boundary conditions into the dimensionless form, the following steps have been implemented as:

$$u = cxf'(\xi) \text{ at } y = 0, \ cxf'(\xi) = cx,$$

$$cxf'(0) = cx, \text{ at } y = 0, \ f'(0) = 1.$$

$$v = -\sqrt{c\nu}f(\xi) \text{ at } y = 0, \ v = -v_0,$$

$$-v_0 = -\sqrt{c\nu}f(\xi), \ v_0 = \sqrt{c\nu}f(0) \text{ at } y = 0, \ f(0) = \frac{v_0}{\sqrt{c\nu}},$$

$$S = \frac{v_0}{\sqrt{c\nu}} \Rightarrow f(\xi) \text{ at } \xi = 0, \ f(0) = S,$$

$$T = T_\infty + Bx^2 \sqrt{\frac{\nu}{c}}\theta(\xi) \text{ at } y = 0, \ \frac{\partial T}{\partial y} = Bx^2,$$

$$\frac{\partial T}{\partial y} = Bx^2 \sqrt{\frac{\nu}{c}}\theta'(\xi).\frac{c}{\nu},$$

$$Bx^2 = Bx^2\theta'(0), \text{ at } y = 0, \ \ \theta'(0) = 1.$$

$$u = 0 \text{ at } y \to \infty, \ \ cxf'(\xi) = 0,$$

$$cxf'(\infty) = 0 \text{ at } y \to \infty, \ f'(\infty) = 0.$$

$$T = T_\infty \text{ at } y \to \infty, \ T = T_\infty + Bx^2\sqrt{\frac{\nu}{c}}\theta(\xi) \text{ at } \ y \to \infty,$$

$$Bx^2\sqrt{\frac{\nu}{c}} = 0, \ \theta(\infty) = 0.$$

The final dimensionless form of the governing equations is:

$$f''' + ff'' - (f'^2 - (M + \lambda)f' = 0, \tag{3.26}$$

$$(1 + \frac{4}{3}R)\theta'' + Prf\theta' - 2Prf'\theta + PrEc\left(f''^2 + Mf'^2\right) - PrQ\theta = 0. \tag{3.27}$$

The transformed boundary conditions (3.3) formulated as:

$$\left.\begin{aligned}
f(0) &= S, \quad f'(0) = 1, \quad \theta'(0) = 1,\\
f(\infty) &= 0, \quad \theta(\infty) = 0.
\end{aligned}\right\} \tag{3.28}$$

In the above equations the dimensionless quantities are formulated as follows.

$$\left.\begin{aligned}
M &= \frac{\sigma B_0^2}{\rho c}, & \lambda &= \frac{\nu}{K_p c},\\
Ec &= \frac{c^{\frac{5}{2}}}{\sqrt{\nu}BC_p}, & Q &= \frac{Q_0}{\rho C_p c},\\
Pr &= \frac{\rho C_p \nu}{k}, & R &= \frac{4\sigma^* T_\infty^3}{k^* k}.
\end{aligned}\right\}$$

3.4   Physical Quantities of Interest

The skin friction coefficient (C_f) and the Nusselt number (Nu_x) are the main physical quantities, we discussed here.

The skin friction coefficient C_f can be expressed as:

$$C_f = \frac{\tau_w}{\rho u_w{}^2},$$

$$\tau_w = \mu \left(\frac{\partial u}{\partial y}\right)_{y=0},$$

$$\frac{\partial u}{\partial y} = cx f''(\xi)\sqrt{\frac{c}{\nu}},$$

$$C_f = \mu \left(\frac{cx\sqrt{\frac{c}{\nu}} f''(0)}{\rho c^2 x^2}\right),$$

$$C_f = \frac{\sqrt{\nu}}{\sqrt{cx}} f''(0),$$

$$C_f = \frac{1}{\sqrt{Re}} f''(0),$$

$$Re^{\frac{1}{2}} C_f = f''(0).$$

Mathematical form of the Nusselt number Nu_x is

$$Nu_x = \frac{x q_w}{k(T_w - T_\infty)},$$

$$q_w = \left(-\left(k + \frac{16\sigma^* T_\infty^3}{3k^*}\right)\left(\frac{\partial T}{\partial y}\right)\right)_{y=0},$$

$$Nu_x = \frac{-x\left(k + \frac{16\sigma^* T_\infty^3}{3k^*}\right) Bx^2}{k\left(Bx^2\sqrt{\frac{\nu}{c}}\theta(\xi)\right)},$$

$$Nu_x = \frac{-Bx^3\left(k + \frac{16\sigma^* T_\infty^3}{3k^*}\right)}{Bx^2\left(k\sqrt{\frac{\nu}{c}}\right)\theta(0)},$$

$$Nu_x = \frac{-\sqrt{\frac{c}{\nu}}x\left(1 + \frac{4}{3}R\right)}{\theta(0)},$$

$$Nu_x = \frac{-Re^{\frac{1}{2}}\left(1 + \frac{4}{3}R\right)}{\theta(0)},$$

$$Re^{\frac{-1}{2}} Nu_x = -\frac{1 + \frac{4}{3}R}{\theta(0)}.$$

where, the local Reynolds number is: $Re_x = \frac{u_w x}{\nu}$.

3.5 Solution Methodology

To obtain the numerical solution for the system of ordinary differential equations (3.26) and (3.27) subject to boundary conditions Eq. (3.28), the shooting method with RK4 has been used. First, the momentum equation is solved independently. Following notations have been considered for the conversion of these equation into a system of first order differential equations as follows:

$$f = g_1, \quad f' = g_1' = g_2, \quad f'' = g_2' = g_3, \quad f''' = y_1''' = y_2'' = y_3'.$$

Rewriting these representations with initial conditions, as a result the momentum equation is converted into following system of first order ODEs.

$$g_1' = g_2; \qquad\qquad\qquad\qquad g_1(0) = S,$$
$$g_2' = g_3; \qquad\qquad\qquad\qquad g_2(0) = 1,$$
$$g_3' = (g_1 g_3) + g_2{}^2 + (M + \lambda)g_2; \qquad\qquad g_3(0) = \chi.$$

where χ is the missing initial condition. The IVP has been solved by using RK4 method.

The domain of the IVP has been taken as $[0, \xi_\infty]$ instead of $[0, \infty)$. Where ξ_∞ ia chosen in such a way that no significant variation is observed in the solution for $\xi > \xi_\infty$.

The missing condition χ is to be chosen such that, the component g_2 satisfies the follow boundary condition.

$$g_2(\xi_\infty, \chi) = 0.$$

To solve the above equation, Newton's method is used to refine the value of χ with following iterative scheme.

$$\chi_{j+1} = \chi_j - \frac{g_2(\xi_\infty, \chi_j)}{\frac{\partial}{\partial \chi}(g_2(\xi_\infty, \chi_j))}, \qquad\qquad j = 0, 1, 2, 3, \ldots.$$

We further introduce the following notations,

$$\frac{\partial g_1}{\partial \chi} = g_4, \qquad \frac{\partial g_2}{\partial \chi} = g_5, \qquad \frac{\partial g_3}{\partial \chi} = g_6.$$

Hence the Newton's iterative scheme gets the following form

$$\chi_{j+1} = \chi_j - \frac{g_2(\xi_\infty, \chi_j)}{g_5(\xi_\infty, \chi_j)}, \qquad j = 0, 1, 2, 3, \ldots.$$

Now differentiating the system of first order ODEs with respect to χ, three more equations will be appeared.

$$g_4' = g_5; \qquad\qquad\qquad g_4(0) = 0,$$
$$g_5' = g_6; \qquad\qquad\qquad g_5(0) = 0,$$
$$g_6' = -\left(g_1 g_6 + g_4 g_3\right) + 2 g_2 g_5 + (M + \lambda)\, g_5; \qquad g_6(0) = 1.$$

The stoping criteria for the Newton's method is set as. The Newton's iterative process is repeated until the following condition is met.

$$|g_2(\xi_\infty, \chi)| < \epsilon,$$

here ϵ is taken as 10^{-6}.

To numerically solve the Eq. (3.27), the missing condition at $\theta(0)$ is q.
The following representations are considered:

$$\theta = H_1, \qquad \theta' = H_2, \qquad \theta'' = H_2'.$$

As a result, the energy equation (3.27) is converted into the following system of first order ODEs.

$$H_1' = H_2; \qquad\qquad\qquad\qquad\qquad\qquad H_1(0) = q,$$
$$H_2' = \frac{1}{1 + \frac{4}{3}R} \left(-Pr g_1 H_2 + 2 Pr g_2 H_1 - Pr Ec\left(g_3^2 + M g_2^2\right) + Pr Q H_1\right); \quad H_2(0) = 1.$$

The above IVP will be numerically solved by RK4 technique. In the above initial value problem, the missing condition q is satisfy the following relation.

$$H_1(\xi_\infty, q) = 0.$$

The above equation can be solved by using Newton's method with the following iterative formula.

$$q_{j+1} = q_j - \frac{H_2(\xi_\infty, q)}{H_2{}'(\xi_\infty, q)}.$$

We further introduce the following notations,

$$\frac{\partial H_1}{\partial q} = H_3, \qquad \frac{\partial H_2}{\partial q} = H_4.$$

Now differentiating the system of two first order ODEs with respect to q, we get another system of ODEs, as follows.

$$H_3' = H_4; \qquad\qquad\qquad H_3(0) = 1,$$

$$H_4' = \frac{1}{1 + \frac{4}{3}R} \left(-Prg_1 H_4 + 2Prg_2 H_3 + PrQH_3 \right); \qquad H_4(0) = 0.$$

The stopping criteria for the Newton's method is set as.

$$\{|H_1(\xi_\infty, q)|\} < 10^{-6}.$$

3.6   Results and Discussion

In this section, the numerical results have been displayed in the form of graphs and tables. Computations are conducted for different values of the magnetic parameter M, permeability parameter λ, suction and injection parameter S, Radiation parameter R, Prandtl number Pr, Eckert number Ec, heat generation parameter Q and impact of these parameters on velocity and temperature profiles are debated. In Figure 3.2 it is clear that velocity profile decreases with the enhancing value of M. Increasing value of M creates the lorentz force and collision between the conducting molecules increases in the presence of this force due to which temperature of the fluid increases. The effects of the permeability parameter λ on

velocity profile $f'(\xi)$ are depicted in Figure 3.3. It is clear that velocity profile is decreasing by increasing the value of λ. It is comprehensively known that the expansion of permeable material within the stream causes a drag force, causing the stream to slow down. The impacts of magnetic parameter M on temperature profile $\theta(\xi)$ are depicted in Figure 3.4. It is clear that temperature profile increasing by increasing the value of M, due to Lorentz force admitted by the magnetic field in the flow region temperature rises with magnetic parameter. In Figure 3.5 with the increasing permeability parameter λ the fluid temperature rises in case of $(S = -0.5)$ and $(S = 0.5)$. As addition of permeable material in the flow causes a drag force, causing the flow to slow down and temperature of the fluid increases. Figure 3.6 demonstrates that if the value of Radiation parameter R enhances, the temperature profile also increase and heat energy will be liberated to the fluid. so, greater value of R elaboration takes place in the temperature profile. Figure 3.7 shows that if we increases the values of Prandtl number Pr the distribution of Heat is transferred away from the hot surface is steady. When the values of Pr declines the dispersing of heat away from the heated surface is fast. Hence temperature profile decreases with increasing of Prandtl number values. In Figure 3.8 it has been found that Increasing the value of Ec the temperature profile reduced. If the value of Ec is positive, it causes cooling of the sheet. physically $Q > 0$ demonstrates $T_w > T_\infty$, which involves the supply of heat to the flow from the wall. Therefore, if the value of Q increases in the existence of $(S = -0.5)$ and suction $(S = 0.5)$ the temperature profile declines as shown in Figure 3.9.

The influence of various effective parameters on the skin friction coefficient C_f and the local Nusselt number $Nu_x Re_x^{\frac{-1}{2}}$ is shown in Tables 3.1 and 3.2.

In Table 3.1 for the rising the value of M and λ, local Nusselt number $Nu_x Re_x^{\frac{-1}{2}}$ and skin friction coefficient $C_f Re_x^{\frac{1}{2}}$ are decreases. For the rising value of radiation parameter R, Prandtl number Pr, Eckert number Ec and Q, the local Nusselt number $Nu_x Re_x^{\frac{-1}{2}}$ increases for $S = -0.5$. Table 3.2 shows the behaviour of local Nusselt number $Nu_x Re_x^{\frac{-1}{2}}$ and skin friction coefficient $C_f Re_x^{\frac{1}{2}}$ for various parameter. For increasing the value of M, Nusselt number $Nu_x Re_x^{\frac{-1}{2}}$ increases and the skin friction coefficient $C_f Re_x^{\frac{1}{2}}$ decreases. For rising the value of λ local Nusselt

number and the skin friction coefficient are found to decrease. It can be observed that the local Nusselt number increases for larger values of radiation parameter R, Prandtl number Pr, Eckert number Ec and Q for $S = 0.5$.

TABLE 3.1: Calculated values for the skin friction coefficient and Nusselt number for $S = -0.5$ and different values of various parameter given below.

| M	λ	R	Pr	Ec	Q	Present		Ref. [42]	
						$-\mathbf{C_f Re_x^{\frac{1}{2}}}$	$\mathbf{Nu_x Re_x^{\frac{-1}{2}}}$	$-\mathbf{C_f Re_x^{\frac{1}{2}}}$	$\mathbf{Nu_x Re_x^{\frac{-1}{2}}}$
0.0	0.1	0.1	0.72	0.2	0.2	0.828243	1.124318	0.828193	1.122511
0.5						1.039380	1.101820	1.039380	1.101777
0.7						1.114734	1.094640	1.114734	1.094561
0.5	0.0					1.000002	1.110644	1.114734	1.110629
	0.3					1.1147346	1.085531	1.000000	1.085220
	0.5					1.186140	1.070166	1.114734	1.070016
	0.1	0.0				1.186140	1.047671	1.186141	1.048135
		0.3				1.186140	1.198052	1.186141	1.197294
		0.5				1.186140	1.282295	1.186141	1.280275
		0.1	0.5			1.186140	0.883259	1.186141	0.882080
			0.8			1.186140	1.173445	1.186141	1.173573
			1.0			1.186140	1.338949	1.186141	1.339317
			0.72	0.1		1.186140	1.064542	1.186141	1.064425
				0.5		1.186140	1.2311610	1.186141	1.231380
				1.0		1.186140	1.530620	1.186141	1.531700
				0.2	0.1	1.186140	1.05190	1.186141	1.051023
					0.5	1.186140	1.229588	1.186141	1.229901
					1.0	1.186140	1.404916	1.186141	1.405220
	0.3		0.3			1.134546	1.085931	1.098765	1.095220
	0.5		0.4			1.139876	1.089031	1.087600	1.198720
0.0		0.2				1.108946	1.085531	1.897611	1.197294
0.3			0.5			1.118976	1.1908531	1.8909786	1.112020
	0.1	0.5				1.186140	1.047671	1.186141	1.048135
					0.3	1.196140	1.213958	1.196141	1.219901

TABLE 3.2: Calculated values for the skin friction coefficient and Nusselt number for $S = 0.5$ and different values of various parameter given below.

M	λ	R	Pr	Ec	Q	\multicolumn{2}{c}{Present}		\multicolumn{2}{c}{Ref. [42]}	
						$-\mathbf{C_f Re_x^{\frac{1}{2}}}$	$\mathbf{Nu_x Re_x^{\frac{-1}{2}}}$	$-\mathbf{C_f Re_x^{\frac{1}{2}}}$	$\mathbf{Nu_x Re_x^{\frac{-1}{2}}}$
0.0	0.1	0.1	0.72	0.2	0.2	1.328199	1.475153	1.328193	1.475553
0.5						1.539379	1.475482	1.539380	1.476072
0.7						1.614734	1.476335	1.614734	1.476997
0.5	0.0					1.500000	1.480848	1.499999	1.481418
	0.3					1.614734	1.465576	1.614734	1.466203
	0.5					1.686140	1.456625	1.686141	1.457288
	0.1	0.0				1.539379	1.440848	1.686141	1.441541
		0.3				1.539379	1.539490	1.686141	1.539609
		0.5				1.686140	1.597529	1.686141	1.596651
		0.1	0.5			1.686140	1.104356	1.686141	1.103911
			0.8			1.686140	1.606845	1.686141	1.607602
			1.0			1.686140	1.930757	1.686141	1.931816
			0.72	0.1		1.686140	1.399879	1.686141	1.400248
				0.5		1.686140	1.760762	1.686141	1.762364
				1.0		1.686140	2.597935	1.686141	2.604196
				0.2	0.1	1.686140	1.422290	1.686141	1.422651
					0.5	1.686140	1.612618	1.686141	1.613325
					1.0	1.686140	1.799781	1.686141	1.800472
0.0	0.3					1.614734	1.465576	1.614734	1.466203
	0.5					1.696140	1.476625	1.696141	1.497288
	0.2					1.519379	1.450848	1.526141	1.451541
		0.3				1.539379	1.539490	1.686141	1.539609
0.3		0.7				1.686140	1.597529	1.686141	1.596651
		0.1	0.5			1.686140	1.104356	1.686141	1.103911
			0.8			1.686140	1.606845	1.686141	1.607602
			1.0			1.686140	1.930757	1.686141	1.931816
			0.72	0.1		1.686140	1.399879	1.686141	1.400248
				0.5		1.686140	1.760762	1.686141	1.762364
		0.3				1.539379	1.539490	1.686141	1.539609
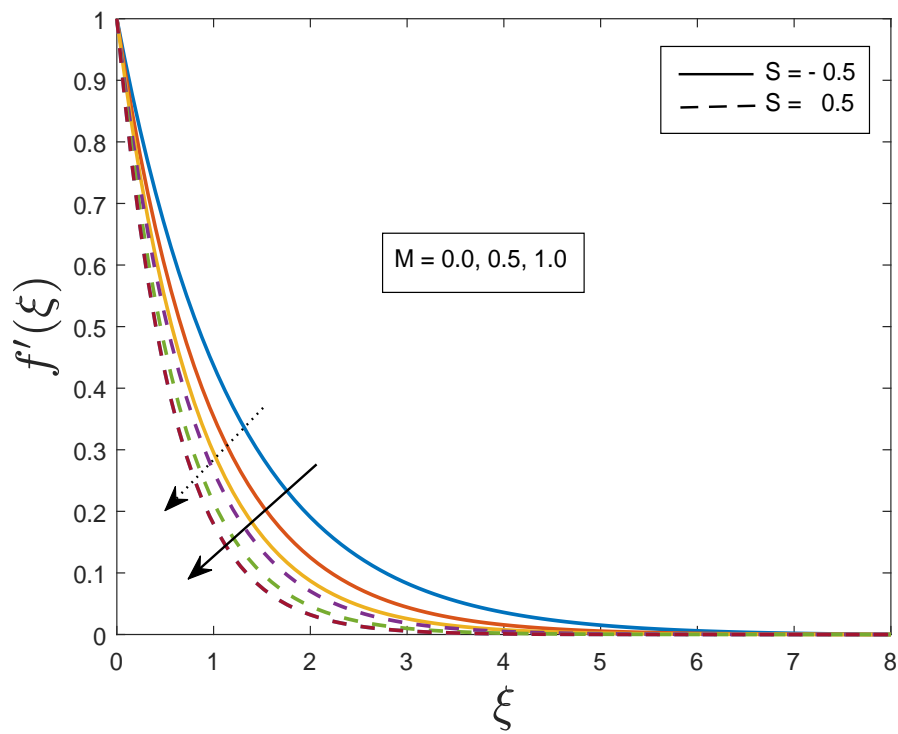
FIGURE 3.2: Effect of M on $f'(\xi)$.
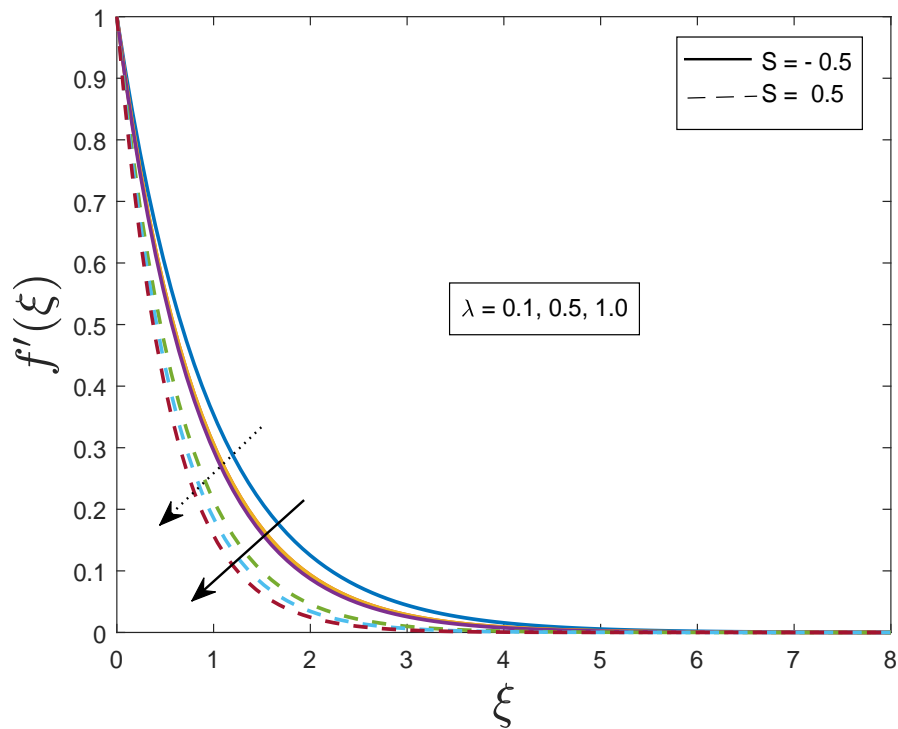
FIGURE 3.3: Effect of λ on $f'(\xi)$.
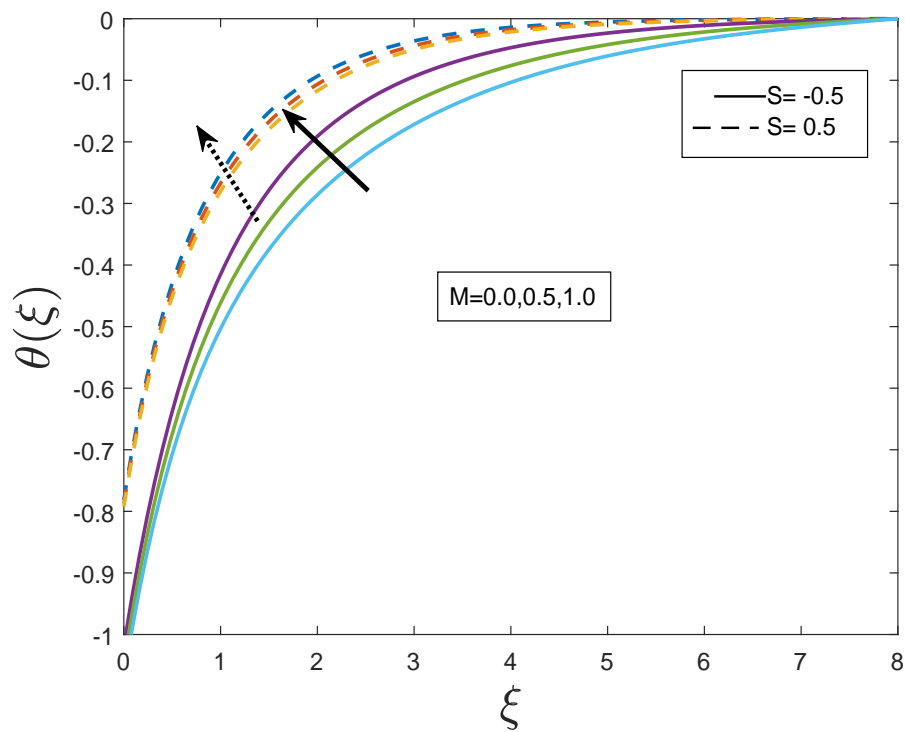
FIGURE 3.4: Effect of M on $\theta(\xi)$.
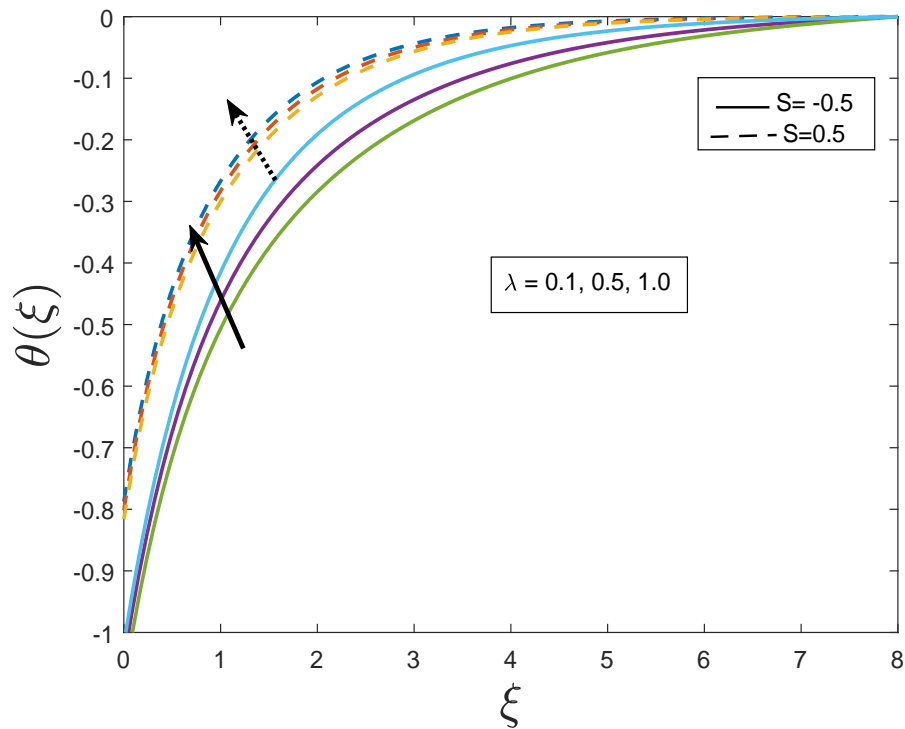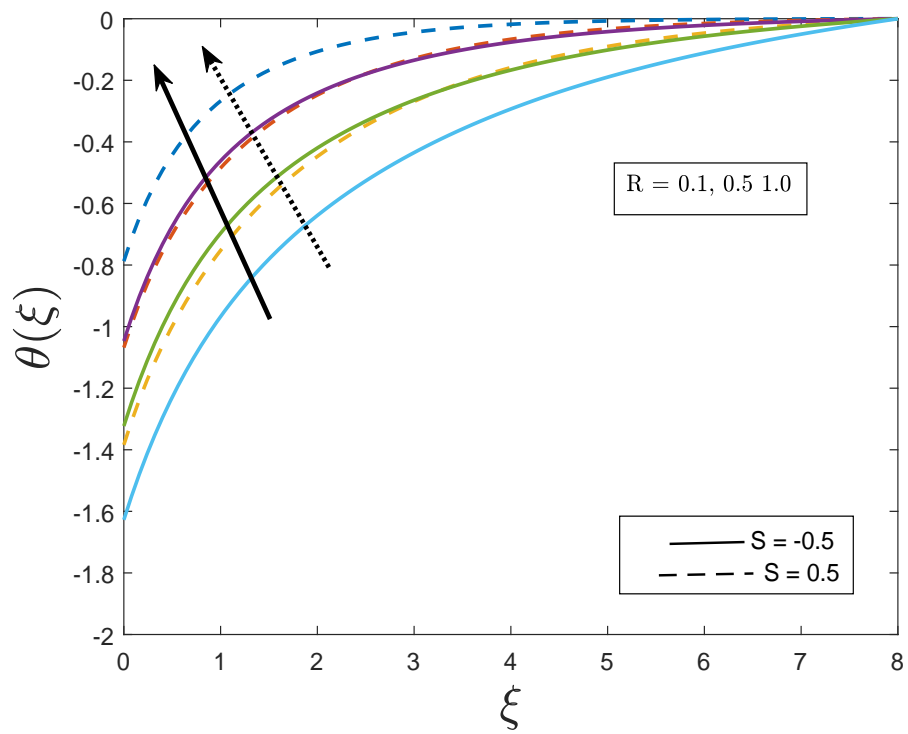

FIGURE 3.5: Effect of λ on $\theta(\xi)$.
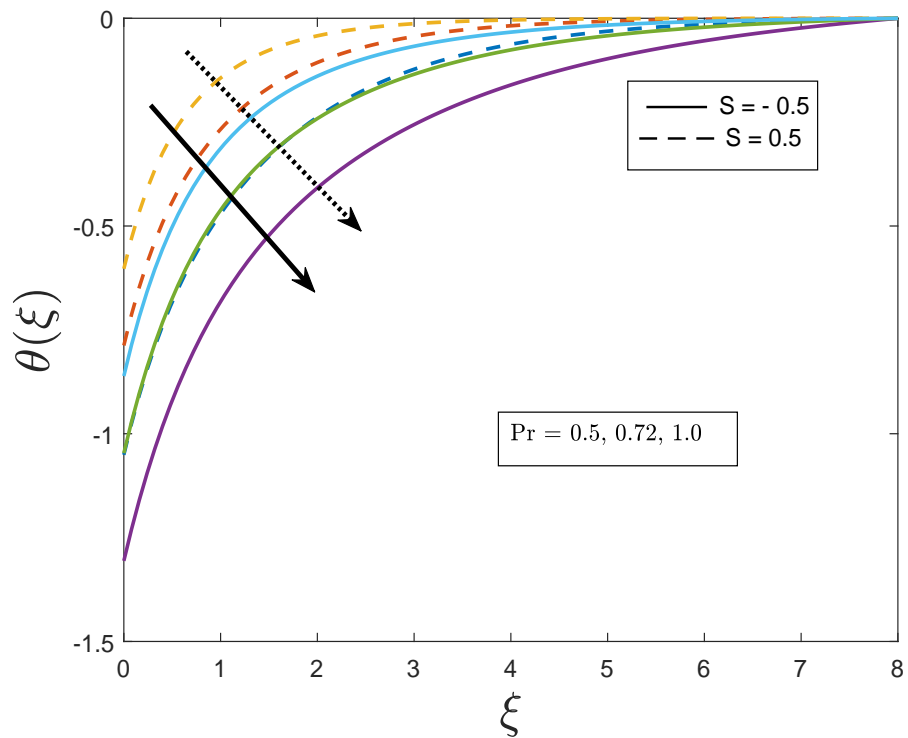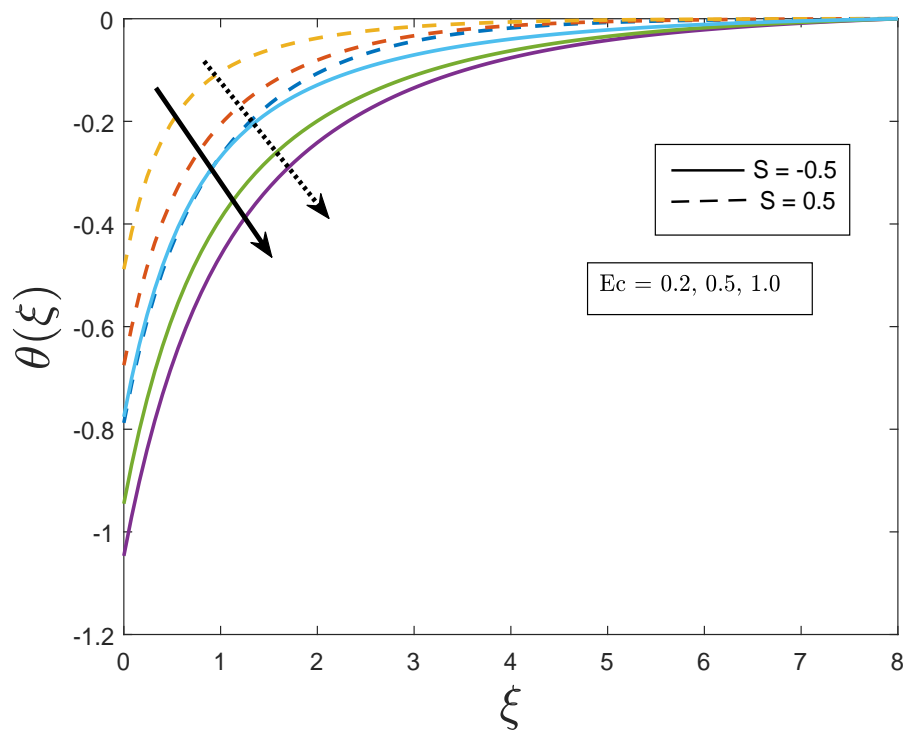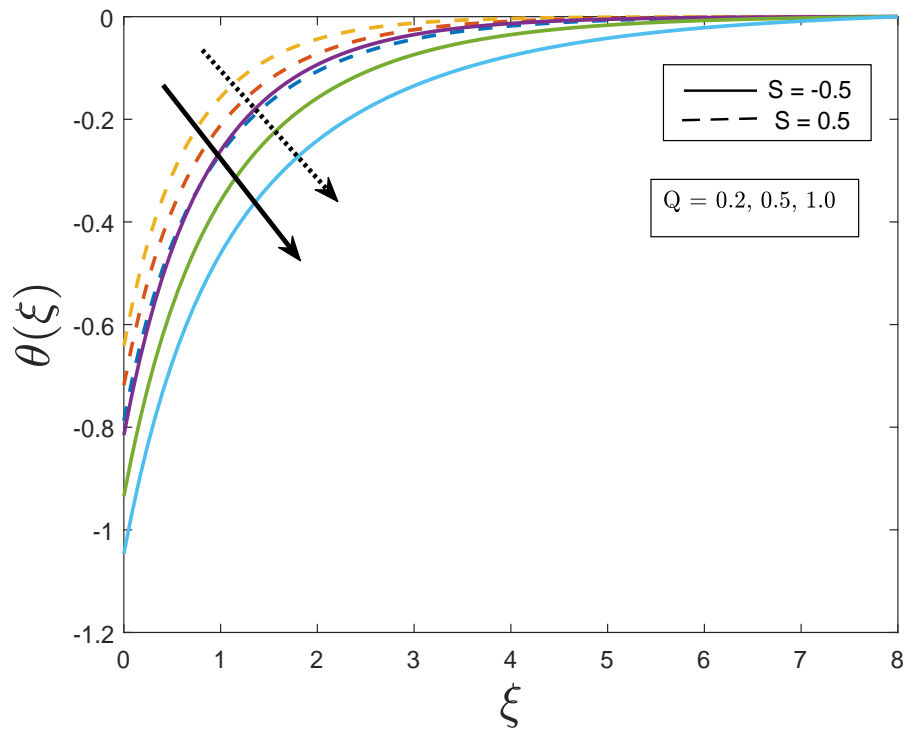
FIGURE 3.6: Effect of R on $\theta(\xi)$.

FIGURE 3.7: Effect of Pr on $\theta(\xi)$.

FIGURE 3.8: Effect of Ec on $\theta(\xi)$.

FIGURE 3.9: Impact of Q on $\theta(\xi)$.

Chapter 4

Impact of Tangent Hyperbolic Fluid and Chemical Reaction on Radiative MHD Flow

The article of Ibrahim [42] reviewed in the preceding chapter has been extended by considering the impact of viscous dissipation of tangent hyperbolic fluid and chemical reaction rate. By using the similarity variables, the governing non-linear PDEs are converted into ODEs. By using shooting technique, the solution of ordinary differential equations is obtained. At the end of this chapter, the impact of various parameters of the transformed ODEs is discussed for dimensionless velocity, temperature, concentration, Nusselt number, skin friction coefficient and Sherwood mumber. Investigation of numerical results is presented through the graphs and tables.

4.1   Mathematical Modeling

Consider a steady, two dimensional, radiative MHD flow of an incompressible tangent hyperbolic viscous fluid over a permeable extending sheet placed at $y{=}0$ in the existence of Joule heating and viscous dissipation. The direction of the flow

is taken along x-axis while y-axis is considered normal to it. A steady magnetic field of strength B_0 is employed in the perpendicular direction to the sheet. Two equivalent yet inverse strengths follow up on the sheet to extend it along its length with a speed u_w keeping the origin fixed along the x-axis. The velocity of the sheet is assumed to be $u_w = cx$, c is a positive constant. The flow configuration and coordinate system are shown in Figure 4.1. In addition, the concentration of flow is examined with the assistance of concentration equation under the impact of mass diffusion and chemical reaction.
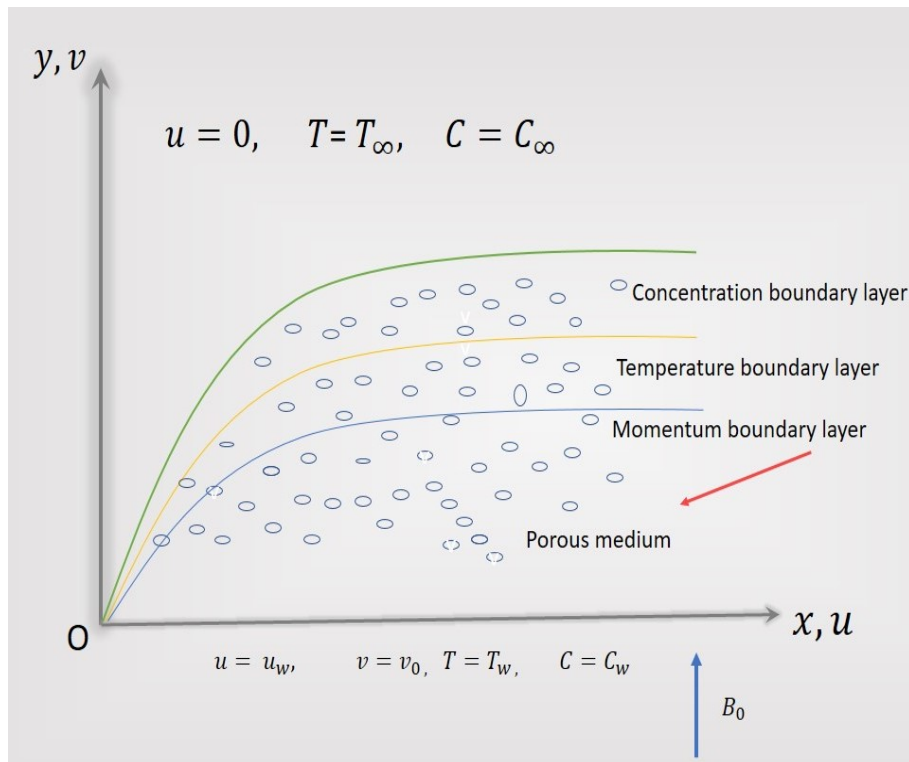

FIGURE 4.1: Physical configuration

4.2   The Governing Equations

With the aforementioned assumptions, the governing equations of the flow are given by

- Continuity Equation:

$$\frac{\partial u}{\partial x} + \frac{\partial v}{\partial y} = 0,\tag{4.1}$$

- Momentum Equation:

$$u\frac{\partial u}{\partial x} + v\frac{\partial u}{\partial y} = \nu(1-n)\frac{\partial^2 u}{\partial y^2} + \sqrt{2}\nu n\Gamma\left(\frac{\partial^2 u}{\partial y^2}\right)\left(\frac{\partial u}{\partial y}\right) - \frac{\sigma B_0^2}{\rho}u - \frac{\nu}{K_p}u,$$

(4.2)

- Energy Equation:

$$u\frac{\partial T}{\partial x} + v\frac{\partial T}{\partial y} = \frac{k}{\rho C_p}\frac{\partial^2 T}{\partial y^2} + \frac{\nu}{C_p}(1-n)\left(\frac{\partial u}{\partial y}\right)^2 + \frac{\nu n\Gamma}{\sqrt{2}C_p}\left(\frac{\partial^2 u}{\partial y^2}\right)\left(\frac{\partial u}{\partial y}\right)$$
$$- \frac{1}{\rho C_p}\frac{\partial q_r}{\partial y} + \frac{\sigma B_0^2}{\rho C_p}u^2 + \frac{Q_0}{\rho C_p}(T_\infty - T).$$

(4.3)

- Concentration Equation:

$$u\frac{\partial C}{\partial x} + v\frac{\partial C}{\partial y} = D\frac{\partial^2 C}{\partial y^2} - K_1(C - C_\infty).$$

(4.4)

Boundary Conditions

The dimensional form of the boundary conditions is given as:

$$\left.\begin{aligned}
&u = cx, \quad v = -v_0, \quad \frac{\partial T}{\partial y} = Bx^2, \ C = C_w, \quad \text{at} \ y = 0,\\
&u = 0, \quad T = T_\infty, \ C = C_\infty, \qquad\qquad \text{at} \ y \to \infty.
\end{aligned}\right\}$$

(4.5)

Here u and v are velocity components in x and y direction, respectively. The x and y are axial and normal coordinates, ρ is the density of the fluid, σ is the electrical conductivity, ν is the kinematic viscosity, k is thermal conductivity, C_p is the specific heat at constant pressure, K_p is the permeability of porous medium, Power law index is denoted by n, D is the mass diffusion, K_1 is the reaction rate on the fluid concentration, T is a fluid temperature, B_0 is magnetic field strength and q_w indicates the wall heat flux.

$$\left.\begin{aligned}
&u = cxf'(\xi), \quad v = -\sqrt{c\nu}f(\xi),\\
&\xi = y\sqrt{\frac{c}{\nu}}, \quad T = T_\infty + Bx^2\sqrt{\frac{\nu}{c}}\theta(\xi),\\
&\phi(\xi) = \frac{C - C_\infty}{C_w - C_\infty}.
\end{aligned}\right\}$$

(4.6)

The detailed procedure for the conversion of Eq. (4.1) into ODE has been discussed in Chapter 3. Now we include the below procedure for the conversion of Eq. (4.2) into the dimensionless form. So in order to derive the left hand side of the Eq. (4.2), the following procedure is adopted.

$$u\frac{\partial u}{\partial x} + v\frac{\partial u}{\partial y} = cxf'(\xi)\frac{\partial}{\partial x}(cxf'(\xi)) + (-\sqrt{c\nu}f(\xi)\frac{\partial}{\partial y}(cxf'(\xi),$$

$$u\frac{\partial u}{\partial x} + v\frac{\partial u}{\partial y} = cxf'(\xi)cf'(\xi) + (-\sqrt{c\nu}f(\xi)\frac{1}{\sqrt{\nu}}c^{\frac{3}{2}}xf''(\xi)),$$

$$u\frac{\partial u}{\partial x} + v\frac{\partial u}{\partial y} = c^2xf'^2(\xi) - c^2xff''. \tag{4.7}$$

Similarly for the derivation of right hand side of Eq. (4.2) following steps are useful

$$\nu(1-n)\frac{\partial^2 u}{\partial y^2} + \sqrt{2}\nu n\Gamma(\frac{\partial^2 u}{\partial y^2})(\frac{\partial u}{\partial y}) - \frac{\sigma B_0^2}{\rho}u - \frac{\nu}{K_p}u, \tag{4.8}$$

$$= \nu(1-n)\frac{c^2x}{\nu}f'''(\xi) + \sqrt{2}\nu n\Gamma\frac{c^2x}{\nu}f'''(\xi)(\frac{c^{\frac{3}{2}}}{\sqrt{\nu}}xf''(\xi)) - (\frac{\sigma B_0^2}{\rho}cxf'(\xi) - \frac{\nu}{K_p}cxf'(\xi). \tag{4.9}$$

By comparing Eq. (4.7) and Eq. (4.9) we get

$$c^2xf'^2(\xi) - c^2xff'' = cx\nu(1-n)\frac{c}{\nu}f'''(\xi) + \sqrt{2}\nu n\Gamma\frac{c}{\nu}f'''(\xi)(\frac{c^{\frac{3}{2}}}{\sqrt{\nu}}xf''(\xi))$$
$$- \frac{\sigma B_0^2}{\rho}f'(\xi) - \frac{\nu}{K_p}f'(\xi),$$

$$\Rightarrow \quad c^2x[f'^2(\xi) - ff''] = cx[\nu(1-n)\frac{c}{\nu}f'''(\xi) + \sqrt{2}\nu n\Gamma x\frac{c}{\nu}f'''(\xi)(\frac{c^{\frac{3}{2}}}{\sqrt{\nu}}xf''(\xi)$$
$$- \frac{\sigma B_0^2}{\rho}f'(\xi) - \frac{\nu}{K_p}f'(\xi)],$$

$$\Rightarrow \quad c[f'^2(\xi) - ff''] = (1-n)cf'''(\xi) + \sqrt{2}\nu n\Gamma x\frac{c^{\frac{5}{2}}}{\sqrt{\nu}}f'''(\xi)f''(\xi))$$
$$- \frac{\sigma B_0^2}{\rho}f'(\xi) - \frac{\nu}{K_p}f'(\xi),$$

$$\Rightarrow \quad f'^2(\xi) - ff'' = (1-n)f'''(\xi) + \sqrt{2}\nu n\Gamma x\frac{c^{\frac{3}{2}}}{\sqrt{\nu}}f'''(\xi)f''(\xi)$$
$$- \frac{\sigma B_0^2}{\rho c}f'(\xi) - \frac{\nu}{K_p c}f'(\xi),$$

$$\Rightarrow \quad f'^2(\xi) - ff'' = (1-n)f'''(\xi) + \sqrt{2}\nu n\Gamma x \frac{c^{\frac{3}{2}}}{\sqrt{\nu}} f'''(\xi)f''(\xi) - Mf'(\xi) - \lambda f'(\xi),$$

$$f'^2(\xi) - ff'' = (1-n)f'''(\xi) + nWef'''(\xi)f''(\xi) - Mf'(\xi) - \lambda f'(\xi). \quad (4.10)$$

Hence the final dimensionless form becomes

$$(1-n)f''' + ff'' - f'^2 - (M + \lambda)f' + nWef'''f'' = 0.$$

Next, converting the energy equation into the dimensionless form we use Eq. (4.6) into Eq. (4.3)

$$T = T_\infty + Bx^2\sqrt{\frac{\nu}{c}}\theta(\xi). \quad (4.11)$$

Differentiating Eq. (4.11) w.r.t 'x' we have

$$\frac{\partial T}{\partial x} = \frac{\partial}{\partial x}\left(Bx^2\sqrt{\frac{\nu}{c}}\theta(\xi)\right),$$

$$\frac{\partial T}{\partial x} = 2Bx\sqrt{\frac{\nu}{c}}\theta(\xi). \quad (4.12)$$

Similarly, differentiating Eq. (4.11) w.r.t 'y'

$$\frac{\partial T}{\partial y} = Bx^2\sqrt{\frac{\nu}{c}}\theta'(\xi)\sqrt{\frac{c}{\nu}},$$

$$\frac{\partial T}{\partial y} = Bx^2\theta'(\xi). \quad (4.13)$$

Now using Eqs. (4.12) and (4.13) into the left hand side of Eq. (4.3)

$$= u\frac{\partial T}{\partial x} + v\frac{\partial T}{\partial y},$$

$$= cxf'(\xi)2Bx\sqrt{\frac{\nu}{c}}\theta(\xi) - \left(\sqrt{c\nu}f(\xi)Bx^2\theta'(\xi)\right),$$

$$= \sqrt{c\nu}f'(\xi)2Bx^2\theta(\xi) - \sqrt{c\nu}f(\xi)Bx^2\theta'(\xi). \quad (4.14)$$

Multiplying Eq. (4.14) by $\frac{\rho C_p}{kBx^2}\sqrt{\frac{\nu}{c}}$

$$= \frac{\rho C_p}{kBx^2}\nu f'(\xi)\theta(\xi)2Bx^2 - \frac{\nu\rho C_p}{k}\theta'(\xi)f(\xi),$$

$$= 2Prf'(\xi)\theta(\xi) - Pr\theta'(\xi)f(\xi). \quad (4.15)$$

Now using Eq. (4.6) into the right hand side of Eq. (4.3), we have

$$
= \frac{k}{\rho C_p} \frac{\partial^2 T}{\partial y^2} + \frac{\nu}{C_p}(1-n)\left(\frac{\partial u}{\partial y}\right)^2 + \frac{\nu n \Gamma}{\sqrt{2}C_p}\left(\frac{\partial^2 u}{\partial y^2}\right)\left(\frac{\partial u}{\partial y}\right)
$$
$$
- \frac{1}{\rho C_p}\frac{\partial q_r}{\partial y} + \frac{\sigma B_0^2}{\rho C_P}u^2 + \frac{Q_0}{\rho C_p}(T_\infty - T),
$$
$$
= \frac{k}{\rho C_p}\frac{\partial^2}{\partial y^2}\left(T_\infty + Bx^2\sqrt{\frac{\nu}{c}}\theta(\xi)\right) + \frac{\nu}{C_p}(1-n)\left(\frac{\partial}{\partial y}(cxf'(\xi))\right)^2
$$
$$
+ \frac{\nu n \Gamma}{\sqrt{2}C_p}\left(\frac{\partial}{\partial y}(cxf'(\xi))\right)\left(\frac{\partial}{\partial y}(cxf'(\xi))\right)^2 - \frac{1}{\rho C_p}\frac{\partial}{\partial y}\left(\frac{-4\sigma^*}{3k^*}\frac{\partial T^4}{\partial y}\right)
$$
$$
+ \frac{\sigma B_0^2}{\rho C_p}(cxf'(\xi))^2 + \frac{Q_0}{\rho C_p}\left(T_\infty - T_\infty - Bx^2\sqrt{\frac{\nu}{c}}\theta(\xi)\right),
$$
$$
= \frac{k}{\rho C_p}\frac{\partial}{\partial y}\left(Bx^2\sqrt{\frac{\nu}{c}}\theta'(\xi)\sqrt{\frac{c}{\nu}}\right) + \frac{1}{\rho C_p}\frac{16}{3}\frac{\sigma^* T^3}{k^*}\frac{\partial^2 T}{\partial y^2} + \frac{\sigma B_0^2}{\rho C_p}c^2x^2 f'^2(\xi)
$$
$$
+ \frac{\nu}{C_p}(1-n)c^2x^2\left(f''(\xi)\right)^2\frac{c}{\nu} + \frac{\nu n \Gamma}{\sqrt{2}C_p}\frac{c^{\frac{3}{2}}x}{\sqrt{\nu}}f''(\xi)c^2x^2\left(f''(\xi)\right)^2\frac{c}{\nu}
$$
$$
+ \frac{Q_0}{\rho C_p}\left(-Bx^2\sqrt{\frac{\nu}{c}}\theta(\xi)\right),
$$
$$
= \frac{k}{\rho C_p}\left(\theta''(\xi)Bx^2\sqrt{\frac{c}{\nu}}\right) + \frac{1-n}{C_p}(c^3x^2)f''^2(\xi) + \frac{\nu n \Gamma}{\sqrt{2}C_p}\frac{c^{\frac{9}{2}}x^3}{\nu\sqrt{\nu}}\left(f''(\xi)\right)^3
$$
$$
+ \frac{1}{\rho C_p}\frac{16}{3}\frac{\sigma^* T^3}{k^*}\theta''(\xi)Bx^2\sqrt{\frac{c}{\nu}} + \frac{\sigma B_0^2}{\rho C_p}c^2x^2 f'^2(\xi) + \frac{Q_0}{\rho C_p}\left(-Bx^2\sqrt{\frac{\nu}{c}}\theta(\xi)\right),
$$
$$
= \frac{k}{\rho C_p}\left(\theta''(\xi)Bx^2\sqrt{\frac{c}{\nu}}\right) + \frac{16\sigma^* T_\infty^3}{\rho C_p 3k^*}\left(\theta''(\xi)Bx^2\sqrt{\frac{c}{\nu}}\right) + \frac{\sigma B_0^2}{\rho C_p}c^2x^2 f'^2(\xi)
$$
$$
+ \frac{Q_0}{\rho C_p}\left(-Bx^2\sqrt{\frac{\nu}{c}}\theta(\xi)\right) + \frac{1-n}{C_p}\left(c^3x^2 f''^2(\xi)\right) + \frac{\nu n \Gamma}{\sqrt{2}C_p}\frac{c^{\frac{9}{2}}x^3}{\nu\sqrt{\nu}}\left(f''(\xi)\right)^3. \quad (4.16)
$$

Multiplying Eq. (4.16) by $\frac{\rho C_p}{kBx^2}\sqrt{\frac{\nu}{c}}$

$$
\Rightarrow \quad \frac{\rho C_p}{kBx^2}\sqrt{\frac{\nu}{c}}\left(\frac{k}{\rho C_p}(\theta''(\xi)Bx^2\sqrt{\frac{c}{\nu}})\right) + \frac{\rho C_p}{kBx^2}\sqrt{\frac{\nu}{c}}\left(\frac{1-n}{C_p}c^3x^2 f''^2(\xi)\right)
$$
$$
+ \frac{\rho C_p}{kBx^2}\sqrt{\frac{\nu}{c}}\left(\frac{\nu n \Gamma}{\sqrt{2}C_p}\frac{c^{\frac{9}{2}}x^3}{\nu\sqrt{\nu}}\left(f''(\xi)\right)^3\right) + \frac{\rho C_p}{kBx^2}\sqrt{\frac{\nu}{c}}\left(\frac{\sigma B_0^2}{\rho C_p}c^2x^2 f'^2(\xi)\right)
$$
$$
- \frac{\rho C_p}{kBx^2}\sqrt{\frac{\nu}{c}}\frac{Q_0}{\rho C_p}\left(Bx^2\sqrt{\frac{\nu}{c}}\theta(\xi)\right) + \frac{\rho C_p}{kBx^2}\sqrt{\frac{\nu}{c}}\left(\frac{16\sigma^* T_\infty^3}{\rho C_P 3k^*}(\theta''(\xi))Bx^2\sqrt{\frac{c}{\nu}}\right),
$$
$$
\Rightarrow \quad \theta''\left(1+\frac{4}{3}R\right) + (1-n)\frac{c^3\rho C_p}{kBC_p}\sqrt{\frac{\nu}{c}}f''^2(\xi) + \frac{\rho C_p}{kBx^2}\sqrt{\frac{\nu}{c}}\left(\frac{\nu n \Gamma}{\sqrt{2}C_p}\frac{c^{\frac{9}{2}}x^3}{\nu\sqrt{\nu}}\left(f''(\xi)\right)^3\right)
$$
$$
+ \frac{\rho C_p \sigma B_0^2 c^2}{kB\rho C_p}\sqrt{\frac{\nu}{c}}f'^2(\xi) - PrQ\theta.
$$

Multiplying and dividing by '$c\nu$'

$$\theta''\left(1+\frac{4}{3}R\right)\frac{c\nu}{c\nu}+(1-n)\frac{c^3\rho C_p}{kBC_p}\sqrt{\frac{\nu}{c}}f''^2(\xi)\frac{c\nu}{c\nu}+nPrEc\frac{c^{\frac{3}{2}}x\Gamma}{\sqrt{2\nu}}\left(f''(\xi)\right)^3$$

$$+\frac{\rho C_p\sigma B_0^2c^2}{kB\rho C_p}\sqrt{\frac{\nu}{c}}\frac{c\nu}{c\nu}f'^2(\xi)-\frac{c\nu}{c\nu}PrQ\theta,$$

$$\theta''(1+\frac{4}{3}R)+(1-n)\,PrEc\left(f''^2\right)+\frac{nPrEcWe}{2}\left(f''(\xi)\right)^3+PrEcMf'^2-PrQ\theta. \tag{4.17}$$

Combining Eq. (4.15) and (4.17)

$$2Prf'(\xi)\theta(\xi)-Pr\theta'(\xi)f(\xi)=\theta''(1+\frac{4}{3}R)+(1-n)\,PrEc\left(f''^2\right)$$

$$+\frac{nPrEcWe}{2}\left(f''(\xi)\right)^3+PrEcMf'^2-PrQ\theta,$$

$$(1+\frac{4}{3}R)\theta''+Pr\theta'(\xi)f(\xi)-2Prf'(\xi)\theta(\xi)+(1-n)\,PrEc\left(f''^2\right)$$

$$+\frac{nPrEcWe}{2}\left(f''(\xi)\right)^3+PrEcMf'^2-PrQ\theta=0.$$

Next, converting the concentration equation into the dimensionless form we use Eq. (4.6) into Eq. (4.4)

$$C=(C_w-C_\infty)\phi(\xi)+C_\infty. \tag{4.18}$$

Differentiate Eq. (4.18) w.r.t $'x'$ we have

$$\frac{\partial C}{\partial x}=(C_w-C_\infty)\phi'(\xi)0,$$
$$u\frac{\partial C}{\partial x}=0. \tag{4.19}$$

Similarly, differentiating Eq. (4.18) w.r.t $'y'$ and multiplying with v

$$\frac{\partial C}{\partial y}=\phi'(C_w-C_\infty)\cdot\sqrt{\frac{c}{\nu}}, \tag{4.20}$$

$$v\frac{\partial C}{\partial y}=\phi'(C_w-C_\infty)\sqrt{\frac{c}{\nu}}\cdot-\sqrt{c\nu}f(\xi), \tag{4.21}$$

$$v\frac{\partial C}{\partial y}=-c(C_w-C_\infty)f(\xi)\phi'(\xi). \tag{4.22}$$

Again differentiating Eq. (4.20) w. r. t. $'y'$

$$\frac{\partial^2 C}{\partial y^2} = \frac{\partial}{\partial y}\left(\phi'(C_w - C_\infty).\sqrt{\frac{c}{\nu}}\right),$$

$$\frac{\partial^2 C}{\partial y^2} = \phi''(C_w - C_\infty)\left(\sqrt{\frac{c}{\nu}}\sqrt{\frac{c}{\nu}}\right),$$

$$\frac{\partial^2 C}{\partial y^2} = \phi''(C_w - C_\infty)\frac{c}{\nu}. \tag{4.23}$$

Now putting Eqs. (4.19), (4.22) and (4.23) in Eq. (4.4), we have

$$0 - c(C_w - C_\infty)f(\xi)\phi'(\xi) = D\phi''(C_w - C_\infty)\frac{c}{\nu} - K_1(C - C_\infty),$$

$$D\frac{c}{\nu}(C_w - C_\infty)\phi'' + c(C_w - C_\infty)f(\xi)\phi'(\xi) - K_1(C - C_\infty) = 0,$$

$$D\frac{c}{\nu}(C_w - C_\infty)\left(\phi'' + \frac{\nu}{D}f\phi(\xi) - \frac{K_1(C - C_\infty)\nu}{D(C_w - C_\infty)c}\right) = 0,$$

$$\phi'' + Scf\phi(\xi) - \frac{K_1((C_w - C_\infty)\phi(\xi) + C_\infty - C_\infty)\nu}{D(C_w - C_\infty)c},$$

$$\phi'' + Scf\phi(\xi) - \frac{K_1\nu}{Dc}\phi(\xi) = 0,$$

$$\phi'' + Scf\phi(\xi) - Sc\gamma\phi(\xi) = 0. \tag{4.24}$$

Next for converting the associated boundary conditions into the dimensionless form, the following steps have been implemented as:

$$u = cxf'(\xi) \text{ at } y = 0, \ cxf'(\xi) = cx,$$

$$cxf'(0) = cx, \text{ at } y = 0, \ f'(0) = 1.$$

$$\tag{4.25}$$

$$v = -\sqrt{c\nu}f(\xi) \text{ at } y = 0, \ v = -v_0,$$

$$-v_0 = -\sqrt{c\nu}f(\xi), \ v_0 = \sqrt{c\nu}f(0) \text{ at } y = 0, \ f(0) = \frac{v_0}{\sqrt{c\nu}},$$

$$S = \frac{v_0}{\sqrt{c\nu}} \Rightarrow f(\xi) \text{ at } \xi = 0, \ f(0) = S.$$

$$T = T_\infty + Bx^2\sqrt{\frac{\nu}{c}}\theta(\xi) \text{ at } y = 0, \ \frac{\partial T}{\partial y} = Bx^2,$$

$$\frac{\partial T}{\partial y} = Bx^2\sqrt{\frac{\nu}{c}}\theta'(\xi).\frac{c}{\nu},$$

$$Bx^2 = Bx^2\theta'(0), \text{ at } y = 0, \ \theta'(0) = 1.$$

$$u = 0 \text{ at } y \to \infty, \quad cxf'(\xi) = 0,$$

$$cxf'(\infty) = 0 \text{ at } y \to \infty, \quad f'(\infty) = 0.$$

$$T = T_\infty \text{ at } y \to \infty, \ T = T_\infty + Bx^2\sqrt{\frac{\nu}{c}}\theta(\xi) \text{ at } \ y \to \infty,$$

$$Bx^2\sqrt{\frac{\nu}{c}} = 0, \ \theta(\infty) = 0.$$

$$C = C_w, \text{ at } y = 0, \ \phi(\xi)(C_w - C_\infty) + C_\infty = C_w,$$

$$\phi(\xi)(C_w - C_\infty) = (C_w - C_\infty),$$

$$\phi(\xi) = 1, \text{ at } \xi = 0, \ \phi(0) = 1.$$

$$C \to C_\infty \text{ at } y \to \infty, \ \phi(\xi)(C_w - C_\infty) + C_\infty \to C_\infty,$$

$$\phi(\xi)(C_w - C_\infty) \to 0, \ \phi(\xi) \to 0 \text{ as } \xi \to \infty, \ \phi(\xi) \to 0.$$

The final non-dimensional form of the governing equations is:

$$(1-n)f''' + ff'' - f'^2 - (M+\lambda)f' + nWef'''f'' = 0, \tag{4.26}$$

$$(1+\frac{4}{3}R)\theta'' + Pr\theta'(\xi)f(\xi) - 2Prf'(\xi)\theta(\xi) + (1-n)\,PrEc\left(f''^2\right)$$
$$+ \frac{nPrEcWe}{2}(f''(\xi))^3 + PrEcMf'^2 - PrQ\theta = 0. \tag{4.27}$$

$$\phi'' + Scf\phi(\xi) - Sc\gamma\phi(\xi) = 0. \tag{4.28}$$

The transformed boundary conditions (4.5) formulated as:

$$\left.\begin{aligned}
f(0) &= S, \ f'(0) = 1, \ \theta'(0) = 1, \ \phi(0) = 1, \\
f'(\infty) &= 0, \quad \phi(\infty) = 0, \quad \theta(\infty) = 0.
\end{aligned}\right\} \tag{4.29}$$

In the above equations the dimensionless quantities are formulated as:

$$M = \frac{\sigma B_0^2}{\rho c} \text{ (Magnetic parameter)},$$

$$\lambda = \frac{\nu}{K_p c} \text{ (Permeability parameter)},$$

$$R = \frac{4\sigma^* T_\infty^3}{k^* k} \text{ (Radiation parameter)},$$

$$S = \frac{v_0}{\sqrt{\nu c}} \text{ (Suction/injection parameter)},$$

$$Ec = \frac{c^{\frac{5}{2}}}{\sqrt{\nu} B C_p} \text{ (Eckert number)},$$

$$Q = \frac{Q_0}{\rho C_p c} \text{ (Heat generation parameter)},$$

$$Pr = \frac{\rho C_p \nu}{k} \text{ (Prandtl number)},$$

$$Sc = \frac{\nu}{D} \text{ (Schmidt number)},$$

$$We = \frac{\sqrt{2} c^{\frac{3}{2}} x \Gamma}{\sqrt{\nu}} \text{ (Weizenberg number)},$$

$$r = \frac{K_1}{c} \text{ (Chemical reaction parameter)}.$$

4.3   Physical Quantities of Interest

The skin friction (C_f), the Nusselt number (Nu_x) and the Sherwood number (Sh_x) are the main physical quantities, we discussed here.

The skin friction coefficient C_f can be expressed as:

$$C_f = \frac{\tau_w}{\rho u_w^2},$$

$$\tau_w = \mu \left(\frac{\partial u}{\partial y} \right)_{y=0},$$

$$\frac{\partial u}{\partial y} = cx f''(\xi) \sqrt{\frac{c}{\nu}},$$

$$C_f = \mu \left(\frac{cx \sqrt{\frac{c}{\nu}} f''(0)}{\rho c^2 x^2} \right),$$

$$C_f = \frac{\nu \sqrt{\frac{c}{\nu}} f''(0)}{cx},$$

$$C_f = \frac{\sqrt{\nu}}{\sqrt{cx}} f''(0),$$

$$C_f = \frac{1}{\sqrt{Re}} f''(0),$$

$$Re^{\frac{1}{2}} C_f = f''(0).$$

The Nusselt number Nu_x

$$Nu_x = \frac{xq_w}{k(T_w - T_\infty)},$$

$$q_w = \left(-\left(k + \frac{16\sigma^* T_\infty^3}{3k^*} \right) \left(\frac{\partial T}{\partial y} \right) \right)_{y=0},$$

$$T = T_\infty + Bx^2 \sqrt{\frac{c}{\nu}} \theta(\xi),$$

$$\left(\frac{\partial T}{\partial y} \right)_{y=0} = Bx^2,$$

$$Nu_x = \frac{-x \left(k + \frac{16\sigma^* T_\infty^3}{3k^*} \right) Bx^2}{k \left(Bx^2 \sqrt{\frac{\nu}{c}} \theta(\xi) \right)},$$

$$Nu_x = \frac{-Bx^3 \left(k + \frac{16\sigma^* T_\infty^3}{3k^*} \right)}{Bx^2 \left(k\sqrt{\frac{\nu}{c}} \right) \theta(0)},$$

$$Nu_x = \frac{-\sqrt{\frac{c}{\nu}} x \left(1 + \frac{4}{3}R \right)}{\theta(0)},$$

$$Nu_x = \frac{-Re^{\frac{1}{2}} \left(1 + \frac{4}{3}R \right)}{\theta(0)},$$

$$Re^{\frac{-1}{2}} Nu_x = -\frac{1 + \frac{4}{3}R}{\theta(0)}.$$

Mathematical form of the Sherwood number is:

$$Sh_x = \frac{-x(\frac{\partial C}{\partial y})_{y=0}}{C_w - C_\infty},$$

$$C = (C_w - C_\infty)\phi(\xi) + C_\infty,$$

$$\frac{\partial C}{\partial y} = \phi'(0)(C_w - C_\infty)\sqrt{\frac{c}{\nu}},$$

$$Sh_x = \frac{-x}{C_w - C_\infty}\phi'(0)\sqrt{\frac{c}{\nu}}(C_w - C_\infty),$$

$$Sh_x = -\sqrt{\frac{xu_w}{\nu}}\phi'(0),$$

$$Sh_x(Re_x)^{\frac{-1}{2}} = -\phi'(0),$$

where, the Reynolds number is: $Re_x = \frac{u_w x}{\nu}$.

4.4   Solution Methodology

To obtain the numerical solution for the dimensionless system of ordinary differential equations (4.26)-(4.28) subject to boundary conditions Eq. (4.29), shooting method with Runge Kutta method of order four has been used. First, the momentum equation is solved independently. Following notations have been considered for the conversion of these equations into a system of first order differential equations as follows:

$$f = y_1, \quad f' = y_1' = y_2, \quad f'' = y_2' = y_3, \quad f''' = y_1''' = y_2'' = y_3'.$$

Rewriting these representations with initial conditions, as a result the momentum equation is converted into following system of first order ODEs.

$$y_1' = y_2; \hspace{6cm} y_1(0) = S, \hspace{1cm} (4.30)$$

$$y_2' = y_3; \hspace{6cm} y_2(0) = 1, \hspace{1cm} (4.31)$$

$$y_3' = \frac{1}{1 - n + nWey_3}[-y_1y_3 + y_2{}^2 + (M + \lambda)y_2]; \hspace{0.5cm} y_3(0) = \alpha. \hspace{0.5cm} (4.32)$$

where α is the missing initial condition. The IVP has been solved by using RK4 method.

The domain of the IVP has been taken as $[0, \xi_\infty]$ instead of $[0, \infty)$. Where ξ_∞ ia chosen in such a way that no significant variation is observed in the solution for $\xi > \xi_\infty$.

The missing condition α is to be chosen such that, the component y_2 satisfies the follow boundary condition.

$$y_2(\xi_\infty, \alpha) = 0.$$

To solve the above equation, Newton's method is used to refine the value of α with following iterative scheme.

$$\alpha_{j+1} = \alpha_j - \frac{y_2(\xi_\infty, \alpha)}{\frac{\partial}{\partial \alpha}(y_2(\xi_\infty, \alpha))}, \hspace{2cm} j = 0, 1, 2, 3, \ldots.$$

We further introduce the following notations,

$$\frac{\partial y_1}{\partial \alpha} = y_4, \qquad \frac{\partial y_2}{\partial \alpha} = y_5, \qquad \frac{\partial y_3}{\partial \alpha} = y_6.$$

Hence the Newton's iterative scheme gets the following form

$$\alpha_{j+1} = \alpha_j - \frac{y_2(\xi_\infty, \alpha)}{y_5(\xi_\infty, \alpha)}, \qquad j = 0, 1, 2, 3, \ldots .$$

By differentiating Eqs. (4.30), (4.31) and (4.32) with respect to α we get three more ODEs.

Thus, we have the following initial value problem (IVP).

$$y_1' = y_2; \qquad\qquad\qquad y_1(0) = S,$$

$$y_2' = y_3; \qquad\qquad\qquad y_2(0) = 1,$$

$$y_3' = \frac{1}{1 - n + nWey_3}[-y_1y_3 + y_2{}^2 + (M + \lambda)y_2]; \qquad y_3(0) = \alpha,$$

$$y_4' = y_5; \qquad\qquad\qquad y_4(0) = 0,$$

$$y_5' = y_6; \qquad\qquad\qquad y_5(0) = 0,$$

$$y_6' = \frac{1}{1 - n + nWey_3{}^2}[1 - n + nWey_3(-y_1y_6 + y_4y_3 + 2y_2y_5$$
$$+ (M + L)y_5) - (y_2^2 - y_1y_3 + (M + \lambda)y_2)nWey_6]; \qquad y_6(0) = 1.$$

The Newton's iterative process is repeated until the following condition is met.

$$|y_2(\xi_\infty, \alpha)| < \epsilon,$$

where ϵ is taken as 10^{-6}.

To numerically solve the Eqs. (4.27) and (4.28), the missing initial condition at $\theta(0)$ is β and $\phi'(0)$ is ζ.

The following representations are considered:

$$\theta = Z_1, \quad \theta' = Z_2, \quad \phi = Z_3, \quad \phi' = Z_4.$$

Using these notations and differentiating the system of four first order ODEs with respect to β, and ζ.

We get another system of ODEs, as follows.

$$Z_1' = Z_2, \qquad\qquad Z_1(0) = \beta,$$

$$Z_2' = \frac{1}{1 + \frac{4}{3}R}[-Pry_1 Z_2 + 2Pry_2 Z_1 - (1 - n)PrEcy_3^2$$
$$- \frac{nPrEcWe}{2}y_3^2 - My_2^2) + PrQZ_1)], \qquad Z_2(0) = 1,$$

$$Z_3' = Z_4, \qquad\qquad Z_3(0) = 1,$$

$$Z_4' = Sc\gamma Z_3 - Scy_1 Z_4, \qquad\qquad Z_4(0) = \zeta,$$

$$Z_5' = Z_6, \qquad\qquad Z_5(0) = 1,$$

$$Z_6' = \frac{1}{1 + \frac{4}{3}R}[-Pry_1 Z_6 + 2Pry_2 Z_5 + PrQZ_5], \qquad Z_6(0) = 0,$$

$$Z_7' = Z_8, \qquad\qquad Z_7(0) = 0,$$

$$Z_8' = Sc\gamma Z_7 - Scy_1 Z_8, \qquad\qquad Z_8(0) = 0,$$

$$Z_9' = Z_{10}, \qquad\qquad Z_9(0) = 0,$$

$$Z_{10}' = \frac{1}{1 + \frac{4}{3}R}[-Pry_1 Z_{10} + 2Pry_2 Z_9 + PrQZ_9], \qquad Z_{10}(0) = 0,$$

$$Z_{11}' = Z_{12}, \qquad\qquad Z_{11}(0) = 0,$$

$$Z_{12}' = Sc\gamma Z_{11} - Scy_1 Z_{12}, \qquad\qquad Z_{12}(0) = 1.$$

The RK4 scheme has been adopted for tackling the above initial value problem. To get the approximate solution, the domain of the problem has been taken as $[0, \xi_\infty]$ instead of $[0, \infty)$, where ξ_∞ is an appropriate finite positive real number as mentioned before. The missing conditions β and ζ in the above system of equations, are to be chosen such that

$$Z_1(\xi_\infty, \beta, \zeta) = 0, \quad Z_4(\xi_\infty, \beta, \zeta) = 0.$$

For the improvement of the missing condition, Newton's method has been implemented which is conducted by following iterative scheme:

$$\begin{bmatrix} \beta^{(j+1)} \\ \zeta^{(j+1)} \end{bmatrix} = \begin{bmatrix} \beta^{(j)} \\ \zeta^{(j)} \end{bmatrix} - \begin{bmatrix} Z_5 & Z_9 \\ Z_8 & Z_{12} \end{bmatrix}^{-1} \begin{bmatrix} Z_1 \\ Z_4 \end{bmatrix} \qquad j = 0, 1, 2, 3, \dots.$$

The stopping criteria for the Newton's method is set as:

$$max\{|Z_1(\xi_\infty)|, |Z_4(\xi_\infty)|\} < \epsilon.$$

4.5   Result and Discussion

The aim of this section is to analyze the numerical results for the velocity, temperature and concentration profiles with the help of graphs and tables by using different values of involved parameter such as magnetic parameter M, permeability parameter λ, suction and injection parameter S, Radiation parameter R, Prandtl number Pr, Eckert number Ec, heat generation parameter Q, Weissenberg number We, power law index n, Schmidt number Sc and γ the chemical reaction rate.

Figure 4.2 represents the impact of permeability parameter on the velocity profile. It is observed that the velocity profile is decreased by increasing the value of permeability parameter. Physically when a porous media is inserted, it creates a drag force. Figure 4.3 shows the effect of magnetic parameter on the velocity profile. It is observed that the velocity profile decreases by enhancing the value of M in the presence of suction and injection, by increasing magnetic parameter a force is produce, which is notable as Lorentz force. With the production of this force a resistive force induces, in opposite to motion of fluid particles. Figure 4.4 represents the impact of power law index n on the velocity profile. It is clear that the velocity profile decreases by increasing the value of n and boundary layer thickness also decreases. Figure 4.5 demonstrates the influence of We on the velocity profile. As We is the ratio of relaxation time of fluid and specific process time. It increases the thickness of the fluid so, velocity profile decreases by enhancing in the value of We. Figure 4.6 demonstrates the influence of M on the concentration profile. By increasing the value of M the concentration an opposing force is produced. The opposing force produces more obstacles in the fluid flow. Figure 4.7 represents the impact of Sc on the concentration profile. As Sc is the ratio of viscous diffusion rate to mass diffusion rate, it is observed that

the concentration profile declines by increasing the value of Sc. The large numerical values Sc produce less mass diffusion therefore nano-particle concentration is dropped. Figure 4.8 demonstrates the influence of chemical reaction rate r on the concentration profile. By increasing the value of chemical reaction parameter r the fluid concentration decreases, it happen because chemical reaction assists to facilitate the transfer of mass and decreases the boundary layer thickness. Figure 4.9 represents the effect of n on the concentration profile. By increasing the value of power law index n tends to accelerate the flow and decreases the boundary layer thickness. Figure 4.10 depicts that the temperature profile increases with the magnetic parameter M. Temperature profile increases because of the resistive force called Lorentz force that crosses the fluid motion and hence heat is transformed. Figure 4.11 delineates the consequence of permeability parameter on the temperature profile. Addition of permeable medium within the flow leads to drag force causing the flow to move slower and liquid temperature rises, hence the temperature profile is enhanced with increasing the permeability parameter. Table 4.1 and 4.2 demonstrate the impact of effective parameters on the local Nusselt number and skin friction coefficient. From these tables, it is observed that Nusselt number increase with the increasing the value of M and λ, increasing value of power law index n and We the value of skin friction also increases. Nusselt number decreases by enhancing the value of Pr. Similarly, for the rising value of M and λ the skin friction coefficient declines and rising Prandtl number Pr values there is no change in skin friction coefficient in case of injection and suction. Table 4.3 represents the impact of various parameter on Sherwood number in case of injection. If the value of M and λ increases the Sherwood number also increases, if we rises the value of We and r there is no change in Sherwood number, increasing the value of Sc and n it will be the escalate in the value of Sherwood number, enhancing the value of Pr, Ec and Q the value of Sherwood number reduced. Table 4.4 shows the influence of different parameter on Sherwood number in the presence of suction. The Sherwood number increases for enhancing the value of M, λ, We and Sc while Sherwood number declines if we enhance the value of r, n and R. By rising the value of Pr, Ec and Q, the Sherwood number is found to decrease.

FIGURE 4.2: Effect of λ on $f'(\xi)$.

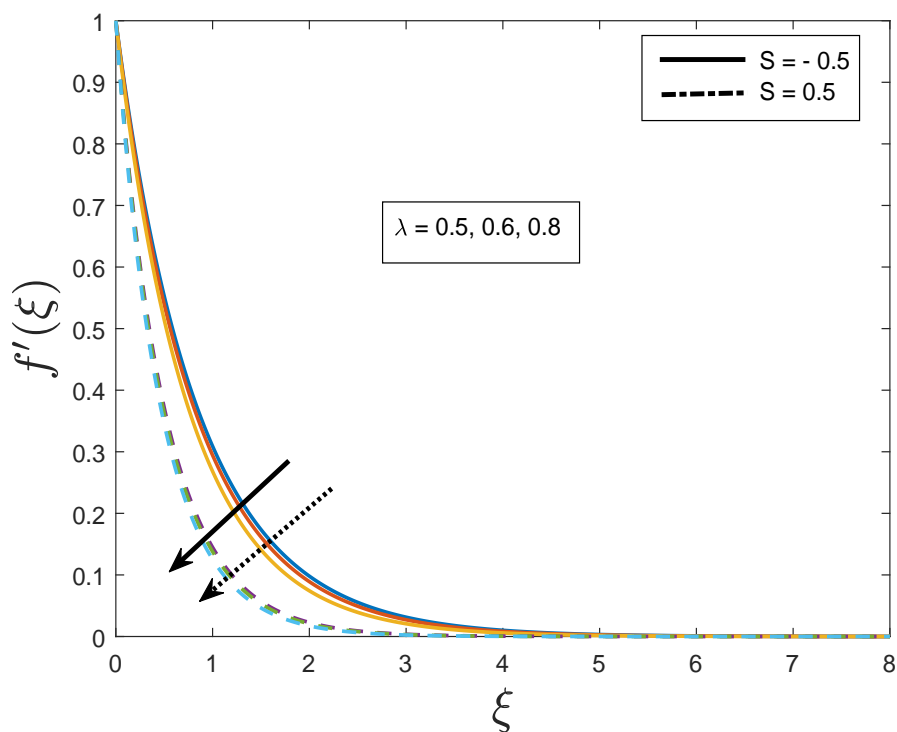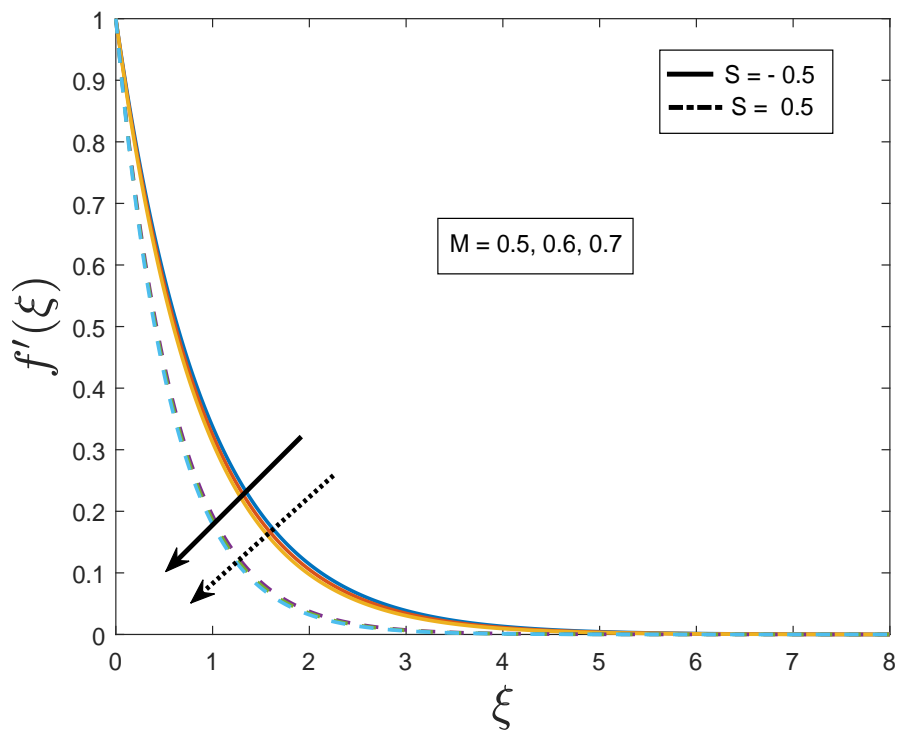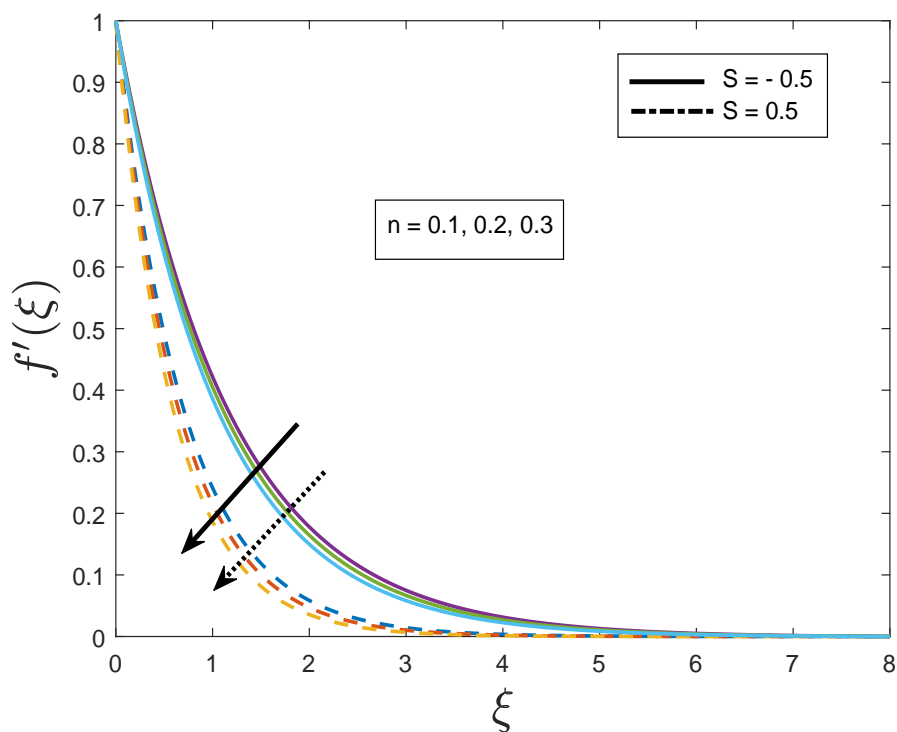FIGURE 4.3: Effect of M on $f'(\xi)$.
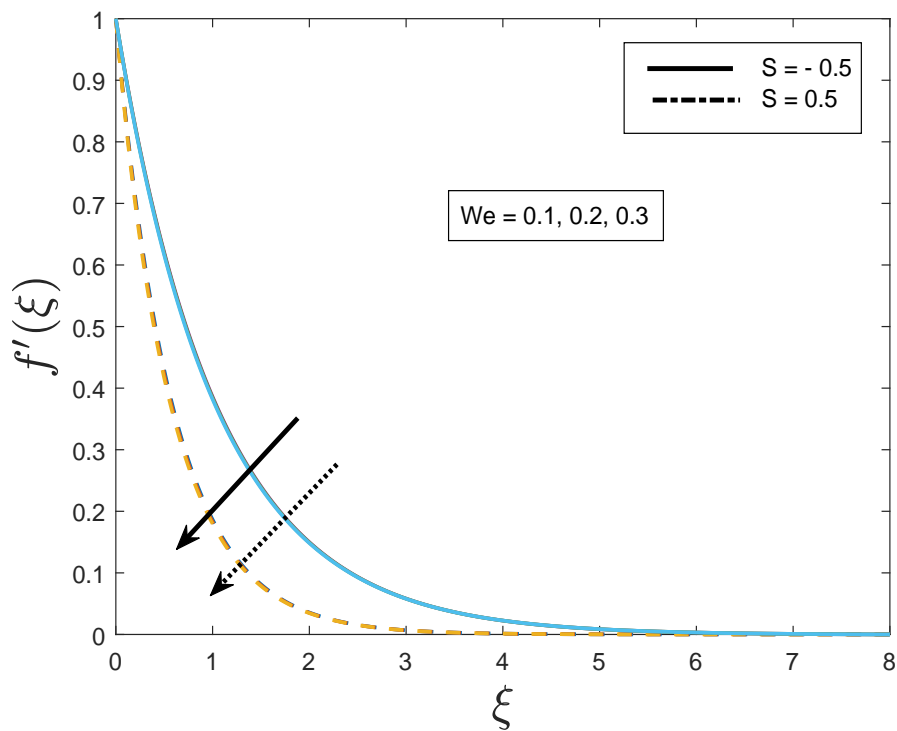
FIGURE 4.4: Effect of n on $f'(\xi)$.

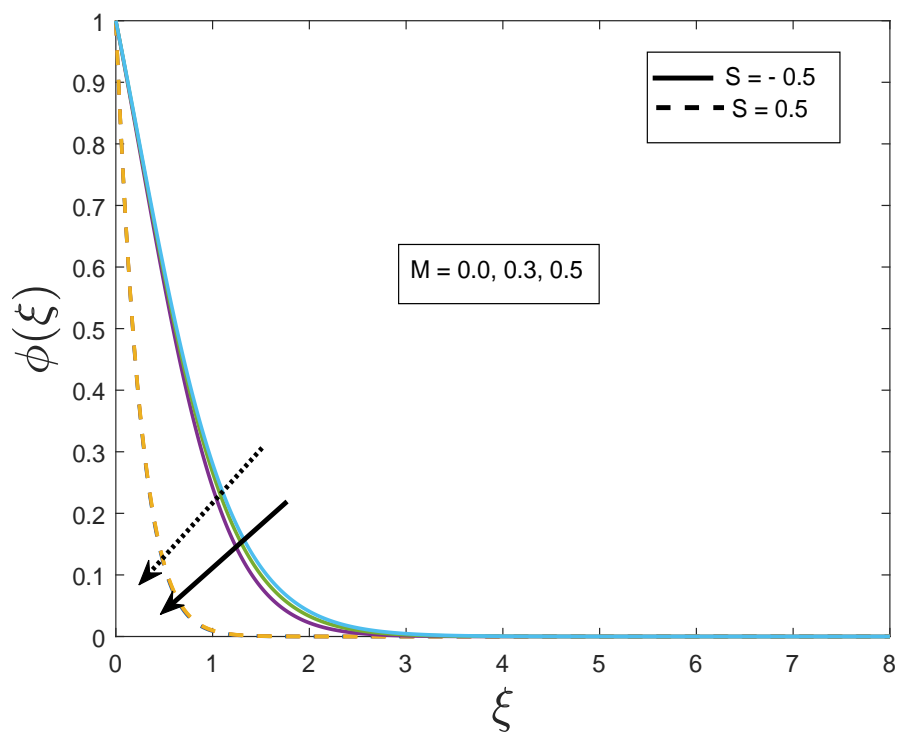FIGURE 4.5: Effect of We on $f'(\xi)$.

FIGURE 4.6: Effect of M on $\phi(\xi)$.
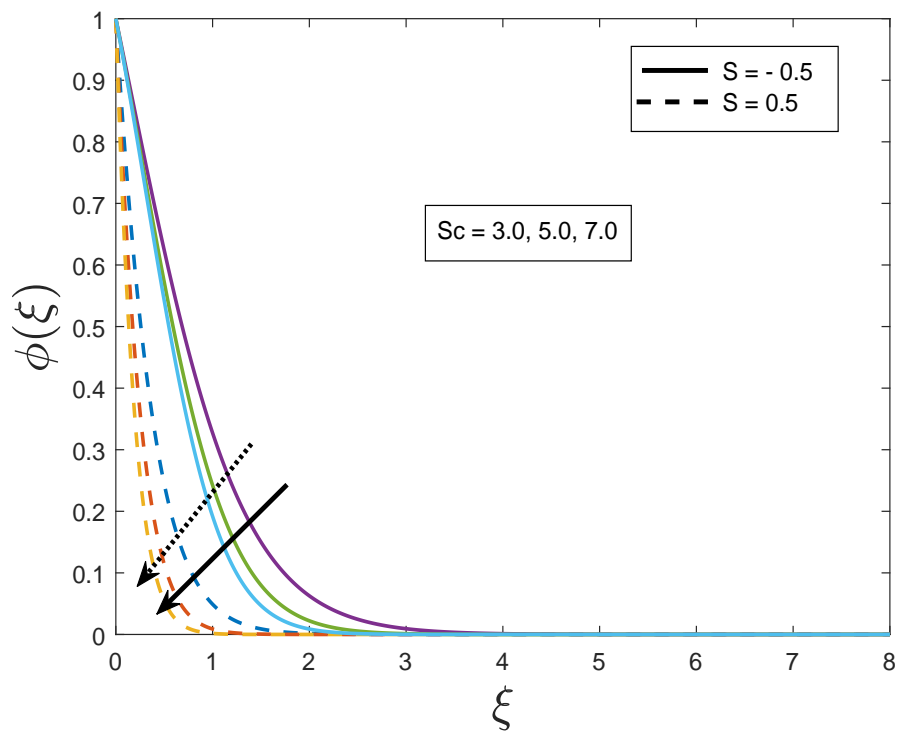
FIGURE 4.7: Effect of Sc on $\phi(\xi)$.
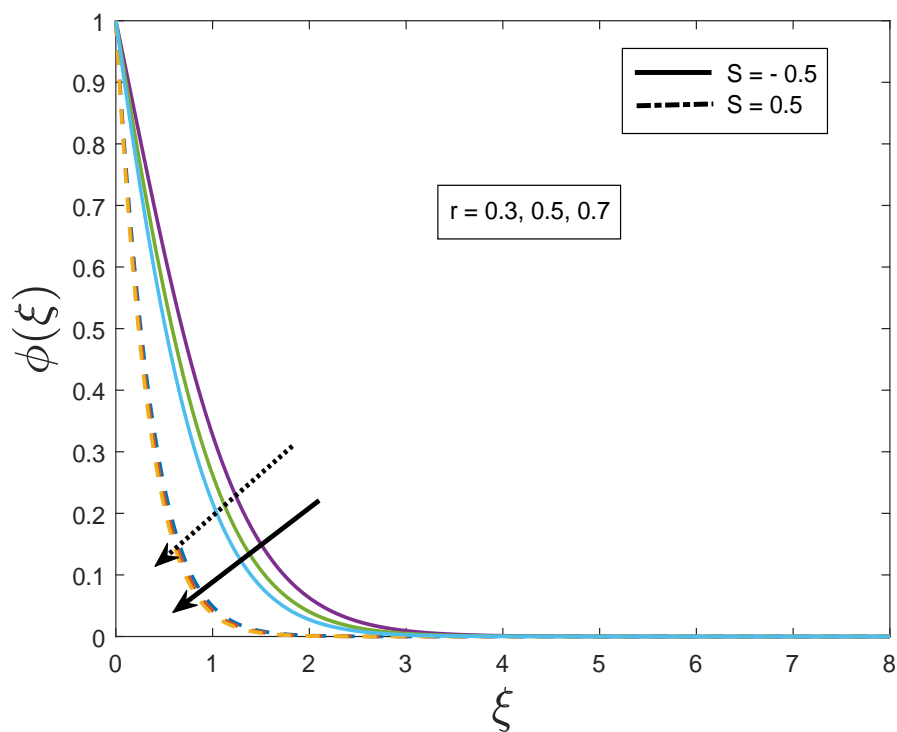
FIGURE 4.8: Effect of r on $\phi(\xi)$.
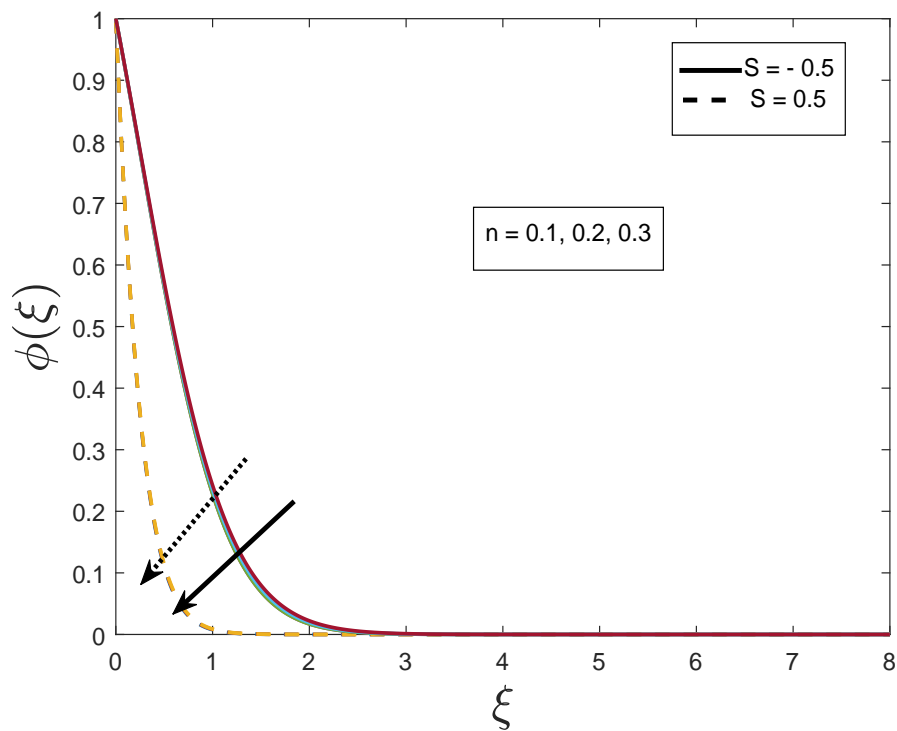
FIGURE 4.9: Effect of n on $\phi(\xi)$.
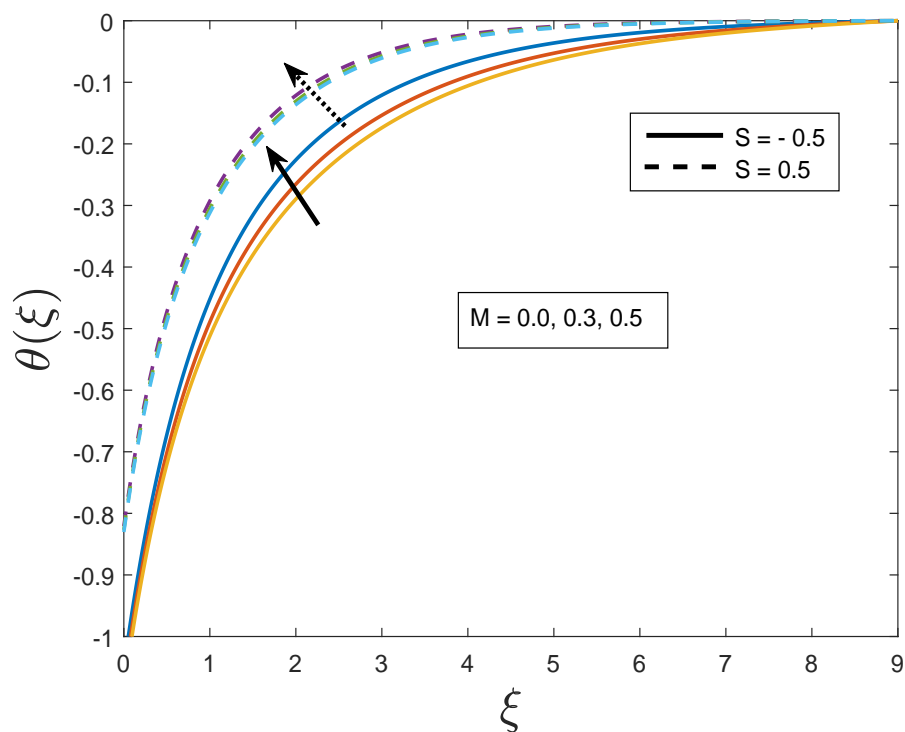
FIGURE 4.10: Effect of M on $\theta(\xi)$.
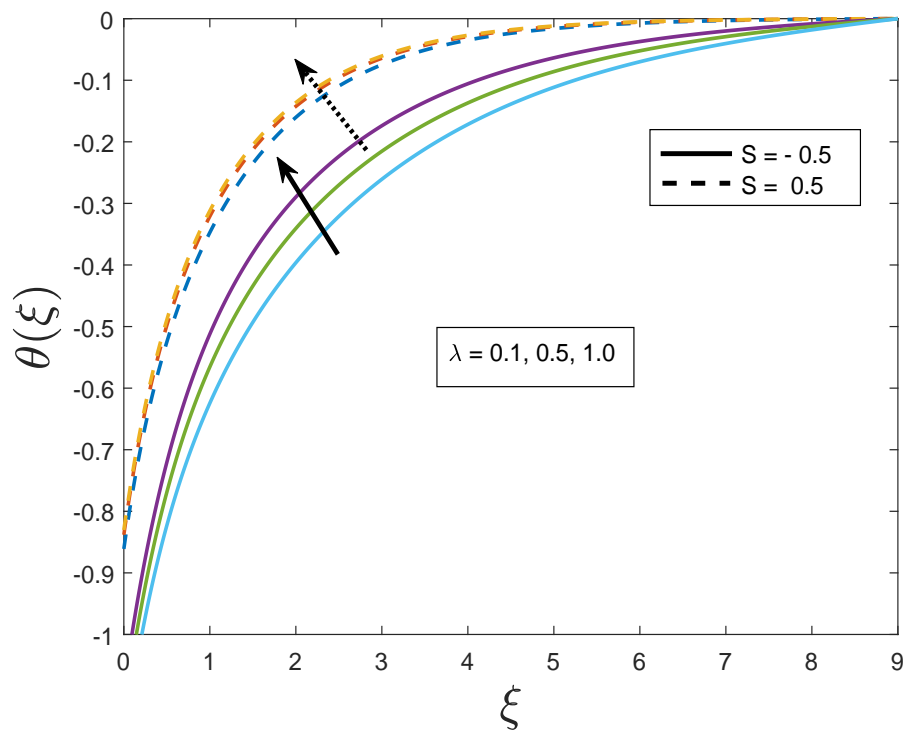
FIGURE 4.11: Effect of λ on $\theta(\xi)$.

TABLE 4.1: Calculated values for skin friction coefficient and Nusselt number for $S = 0.5$ and different values of various parameter given below.

M	λ	We	Sc	γ	n	Pr	Ec	R	Q	$Nu_x Re_x^{\frac{-1}{2}}$	$-C_f Re_x^{\frac{1}{2}}$
0.0	0.1	0.1	5.0	0.3	0.3	0.72	0.2	0.1	0.2	0.80300	1.70769
0.5										0.81261	1.97311
0.7										0.81561	2.06853
0.5	0.0									0.80844	1.92339
	0.3									0.82042	2.06853
	0.5									0.82761	2.15928
								0.0		0.74432	2.15928
								0.3		0.90895	1.97311
	0.1							0.5		1.14218	1.97311
						0.5		0.1		1.09698	1.97311
						0.8				0.74371	1.97311
						1.0				0.61436	1.97311
							0.1			0.65484	1.97311
							0.5			0.49290	1.97311
						0.72	1.0			0.50757	1.97311
									0.1	0.52772	1.97311
									0.5	0.463985	1.97311
				0.7						0.50757	1.97311
				0.9						0.50577	1.97311
			3.0							0.50577	1.97311
			7.0							0.50577	1.97311
					0.1					0.50577	1.97311
					0.2					0.45135	1.650827
		0.3								0.47684	1.790466
		0.5								0.48297	1.85788
				0.4						0.48997	1.93998
0.1				0.6						0.53767	1.97311
			5.0							0.54678	1.97311
			9.0							0.55089	1.97311
									0.2	0.55912	1.97311

TABLE 4.2: Calculated values for skin friction coefficient and Nusselt number for $S = -0.5$ and different values of various parameter given below.

M	λ	We	Sc	γ	n	Pr	Ec	R	Q	$Nu_x Re_x^{\frac{-1}{2}}$	$-C_f Re_x^{\frac{1}{2}}$
0.0	0.1	0.1	5.0	0.3	0.3	0.72	0.2	0.1	0.2	1.03234	0.956399
0.5										1.07041	1.21357
0.7										1.08426	1.30600
0.5	0.0									1.05887	1.165405
	0.3									1.09254	1.30600
	0.5									1.11351	1.39390
									0.0	1.02814	1.39390
									0.3	1.27517	1.39390
	0.1								0.5	1.42701	1.39390
						0.5		0.1		1.34470	1.21357
						0.8				1.00301	1.21357
						1.0				0.87520	1.21357
							0.1			0.90981	1.21357
							0.5			0.77138	1.21357
						0.72	1.0			0.81460	1.21357
								0.1		0.85653	1.21357
								0.5		0.72729	1.21357
				0.7						0.72729	1.21357
				0.9						0.72729	1.21357
			3.0							0.72729	1.21357
			7.0							0.72729	1.21357
					0.1					0.68182	1.08783
					0.2					0.70293	1.14485
		0.3								0.70650	1.16416
		0.5								0.71026	1.18542
				0.4						0.78304	1.49045
0.1				0.6						0.79762	1.50875
			5.0							0.81455	1.06634
			9.0							0.81455	1.06634
									0.2	0.87778	1.06634

TABLE 4.3: Calculated values for Sherwood number for $S = -0.5$ and different values of various parameter given below.

M	λ	We	Sc	γ	n	Pr	Ec	R	Q	$Sh_x Re_x^{\frac{-1}{2}}$
0.0	0.1	0.1	5.0	0.3	0.3	0.72	0.2	0.1	0.2	0.989937
0.3										1.009535
0.5										1.021323
0.7										1.032516
	0.3									1.12004
	0.5									1.040800
	0.7									1.052199
		0.3								0.992600
		0.5								0.995486
		0.7								0.998645
			3.0							0.989937
			7.0							0.989937
			1.0							0.989937
				0.1						0.989937
				0.5						0.989937
				0.7						0.989937
					0.1					0.981729
					0.5					1.016702
					0.3					0.989937
						0.5				1.232902
						0.8				0.930059
						0.72				1.011303
							0.2			0.989937
							0.3			0.968841
							0.5			0.926648
								0.3		1.123496
								0.5		0.989937
									0.2	0.989937

TABLE 4.4: Calculated values for Sherwood number for $S = 0.5$ and different values of various parameter given below.

M	λ	We	Sc	γ	n	Pr	Ec	R	Q	$Sh_x Re_x^{-\frac{1}{2}}$
0.0	0.1	0.1	5.0	0.3	0.3	0.72	0.2	0.1	0.2	0.677254
0.3										0.675594
0.5										0.674256
0.7										0.672771
0.0	0.3									0.6807175
	0.5									0.683674
	0.7									0.686218
	0.1	0.3								0.679135
		0.5								0.6812098
		0.7								0.6836003
		0.1	3.0							0.677254
			7.0							0.677725
			1.0							0.677254
			3.0	0.1						0.677725
				0.5						0.677725
				0.7						0.677725
				0.3	0.1					0.667583
					0.5					0.690033
					0.3					0.677254
					0.3	0.5				0.902587
						0.8				0.621596
						0.72				0.677254
							0.2			0.677254
							0.3			0.643683
							0.5			0.576540
							0.2	0.3		0.896189
								0.5		1.035105
									0.2	0.749723

Chapter 5

Conclusion

In this thesis, the work of Ibrahim et al. [42] is reviewed and extended the radiative MHD flow for the effect of tangent hyperbolic fluid and chemical reaction. First of all, momentum, energy and concentration equations are converted into the ODEs by using appropriate similarity transformations. By using the shooting technique, the numerical solution has been found for the transformed ODEs. To analyze the influence of several physical parameters on velocity, temperature and concentration profiles, the results are presented in the form of tables and graphs. The Skin friction coefficient C_f, Nusselt number Nu_x and Sherwood number Sh_x are investigated through table for the appropriate values of the parameters using MATLAB. The achievements of the current study that has been numerically analyzed, the following worthy points can be concluded:

- The velocity profile decreases by increasing the values of permeability parameter λ, while the temperature profile increases in case of enhancing the value of λ.

- Enhancing the value of Prandtl number, both Nusselt number and temperature profiles declines.

- Sherwood number decreases with higher values of Prandtl and Eckert number, while it increases in case of enhancing the value of the radiation parameter.

- With growth in Schmidt number Sc, the concentration profile declines.

- Velocity profile decreases with an increase in power law index n and Weissenberg number We.

- Skin friction coefficient increases with increasing the values of power law index n and Weissenberg number We.

- The velocity profile deteriorates and temperature profile increases with increasing value of magnetic parameter M.

- Nusselt number increases with enhancing the values of M and λ.

- Skin friction coefficient deteriorates with increasing the values of M and λ.

- Nusselt number depreciates by increasing the values of heat generation parameter.

Bibliography

[1] J. D. McWhirter, M. E. Crawford, and D. E. Klein, "Magnetohydrodynamic flows in porous media II: Experimental results," *Fusion technology*, vol. 34, no. 3P1, pp. 187–197, 1998.

[2] K. Pavlov, "Magnetohydrodynamic flow of an incompressible viscous fluid caused by deformation of a plane surface," *Magnitnaya Gidrodinamika*, vol. 4, no. 1, pp. 146–147, 1974.

[3] C. Geindreau and J. Auriault, "Magnetohydrodynamic flows in porous media," *Journal of fluid mechanics*, vol. 466, p. 343, 2002.

[4] R. Jat and S. Chaudhary, "Magnetohydrodynamic boundary layer flow past a porous substrate with Beavers-Joseph boundary condition," vol. 47, pp. 624–630, 2009.

[5] M. Modather and A. Chamkha, "An analytical study of MHD heat and mass transfer oscillatory flow of a micropolar fluid over a vertical permeable plate in a porous medium," *Turkish Journal of Engineering and Environmental Sciences*, vol. 33, no. 4, pp. 245–258, 2010.

[6] S. Das, R. Jana, and O. Makinde, "Magnetohydrodynamic free convective flow of nanofluids past an oscillating porous flat plate in a rotating system with thermal radiation and hall effects," *Journal of Mechanics*, vol. 32, no. 2, p. 197, 2016.

[7] M. Alim, M. M. Alam, and A. Al-Mamun, "Joule heating effect on the coupling of conduction with magnetohydrodynamic free convection flow from a

vertical flat plate," *Nonlinear Analysis: Modelling and Control*, vol. 12, no. 3, pp. 307–316, 2007.

[8] E. M. Abo-Eldahab and M. A. El Aziz, "Viscous dissipation and Joule heating effects on MHD-free convection from a vertical plate with power-law variation in surface temperature in the presence of Hall and ion-slip currents," *Applied Mathematical Modelling*, vol. 29, no. 6, pp. 579–595, 2005.

[9] M. El-Amin and A. Mohammadein, "Effects of viscous dissipation and Joule heating on magnetohydrodynamic Hiemenz flow of a micropolar fluid," *Heat transfer engineering*, vol. 26, no. 6, pp. 75–81, 2005.

[10] M. Azim, A. Mamun, and M. Rahman, "Viscous Joule heating MHD–conjugate heat transfer for a vertical flat plate in the presence of heat generation," *International Communications in Heat and Mass Transfer*, vol. 37, no. 6, pp. 666–674, 2010.

[11] M. Kayalvizhi, R. Kalaivanan, N. V. Ganesh, B. Ganga, and A. A. Hakeem, "Velocity slip effects on heat and mass fluxes of MHD viscous–ohmic dissipative flow over a stretching sheet with thermal radiation," *Ain Shams Engineering Journal*, vol. 7, no. 2, pp. 791–797, 2016.

[12] S. Chaudhary and M. K. Choudhary, "Heat and mass transfer by MHD flow near the stagnation point over a stretching or shrinking sheet in a porous medium," *Indian Journal of Pure Applied Physics*, vol. 54, pp. 209–217, 2016.

[13] P. Sreenivasulu, T. Poornima, and N. B. Reddy, "Thermal radiation effects on MHD boundary layer slip flow past a permeable exponential stretching sheet in the presence of joule heating and viscous dissipation." *Journal of Applied Fluid Mechanics*, vol. 9, no. 1, 2016.

[14] K. Kaladhar, C. RamReddy, D. Srinivasacharya, and T. Pradeepa, "Analytical study for Soret, Hall, and Joule heating effects on natural convection flow saturated porous medium in a vertical channel," *Mathematical Sciences*, vol. 10, no. 4, pp. 139–148, 2016.

[15] A. Goullieux and J.-P. Pain, "Ohmic heating," in *Emerging technologies for food processing.* Elsevier, 2014, pp. 399–426.

[16] S. K. Ghosh, "Unsteady magnetized flow and heat transfer of a viscoelastic fluid over a stretching surface," *Journal of Magnetism and Magnetic Materials*, vol. 443, pp. 309–318, 2017.

[17] M. Sheikholeslami and D. Ganji, "Nanofluid hydrothermal behavior in existence of lorentz forces considering joule heating effect," *Journal of Molecular Liquids*, vol. 224, pp. 526–537, 2016.

[18] F. Abbasi, T. Hayat, and B. Ahmad, "Numerical analysis for peristalsis of Carreau–Yasuda nanofluid in an asymmetric channel with slip and Joule heating effects," *Journal of Engineering Thermophysics*, vol. 25, no. 4, pp. 548–562, 2016.

[19] M. Waqas, M. Farooq, M. I. Khan, A. Alsaedi, T. Hayat, and T. Yasmeen, "Magnetohydrodynamic MHD mixed convection flow of micropolar liquid due to nonlinear stretched sheet with convective condition," *International Journal of Heat and Mass Transfer*, vol. 102, pp. 766–772, 2016.

[20] M. Khader, "Laguerre collocation method for the flow and heat transfer due to a permeable stretching surface embedded in a porous medium with a second order slip and viscous dissipation," *Applied Mathematics and Computation*, vol. 243, pp. 503–513, 2014.

[21] M. Shojaefard, A. Noorpoor, A. Avanesians, and M. Ghaffarpour, "Numerical investigation of flow control by suction and injection on a subsonic airfoil," *American Jouenel of Applied Mathematics*, vol. 20, pp. 1474–1480, 2005.

[22] O. D. Makinde and T. Chinyoka, "Numerical investigation of buoyancy effects on hydromagnetic unsteady flow through a porous channel with suction/injection," *Journal of Mechanical Science and Technology*, vol. 27, no. 5, pp. 1557–1568, 2013.

[23] S. A. Devi and B. Ganga, "Effects of Viscous and Joules dissipation on MHD flow, heat and mass transfer past a stretching porous surface embedded in a porous medium," *Nonlinear Analysis: Modelling and Control*, vol. 14, no. 3, pp. 303–314, 2009.

[24] A. Hussain, M. Malik, T. Salahuddin, A. Rubab, and M. Khan, "Effects of viscous dissipation on MHD tangent hyperbolic fluid over a nonlinear stretching sheet with convective boundary conditions," *Results in physics*, vol. 7, pp. 3502–3509, 2017.

[25] M. Partha, P. Murthy, and G. Rajasekhar, "Effect of viscous dissipation on the mixed convection heat transfer from an exponentially stretching surface," *Heat and Mass transfer*, vol. 41, no. 4, pp. 360–366, 2005.

[26] S. Mamatha, C. Raju, and G. Madhavi, "Mahesha: Unsteady 3D MHD Carreau and Casson fluids over a stretching sheet with non-Uniform heat source/sink," *Chem. Process Eng. Res*, vol. 52, pp. 10–23, 2017.

[27] M. S. Abel, P. Datti, and N. Mahesha, "Flow and heat transfer in a power-law fluid over a stretching sheet with variable thermal conductivity and non-uniform heat source," *International Journal of Heat and Mass Transfer*, vol. 52, no. 11-12, pp. 2902–2913, 2009.

[28] S. Jyothi, M. S. Reddy, and P. Gangavathi, "Hyperbolic tangent fluid flow through a porous medium in an inclined channel with peristalsis," *International Journal of Advanced Scientific Research and Management*, vol. 1, no. 4, pp. 113–121, 2016.

[29] H. Rumpf, "The characteristics of systems and their changes of state disperse," *Particle Technology, Chapman and Hall; Springer: Berlin/Heidelberg, Germany*, pp. 8–54, 1990.

[30] S. Mansur and A. Ishak, "Unsteady boundary layer flow of a nanofluid over a stretching/shrinking sheet with a convective boundary condition," *Journal of the Egyptian Mathematical Society*, vol. 24, no. 4, pp. 650–655, 2016.

[31] G. Sarojamma and K. Vendabai, "Boundary layer flow of a Casson nanofluid past a vertical exponentially stretching cylinder in the presence of a transverse magnetic field with internal heat generation/absorption," *International Journal of Mathematical and Computational Sciences*, vol. 9, no. 1, pp. 138–143, 2015.

[32] A. Friedman, S. Dyke, and B. Phillips, "Over-driven control for large-scale mr dampers," *Smart materials and structures*, vol. 22, no. 4, p. 045001, 2013.

[33] N. S. Akbar, S. Nadeem, R. U. Haq, and Z. Khan, "Numerical solutions of magnetohydrodynamic boundary layer flow of tangent hyperbolic fluid towards a stretching sheet," *Indian journal of Physics*, vol. 87, no. 11, pp. 1121–1124, 2013.

[34] S. M. Ibrahim, "Effects of mass transfer, radiation, Joule heating and viscous dissipation on steady MHD marangoni convection flow over a flat surface with suction and injection," *International journal of engineering mathematics*, vol. 2013, p. 9, 2013.

[35] M. Hatami, D. Jing, D. Song, M. Sheikholeslami, and D. Ganji, "Heat transfer and flow analysis of nanofluid flow between parallel plates in presence of variable magnetic field using HPM," *Journal of Magnetism and Magnetic Materials*, vol. 396, pp. 275–282, 2015.

[36] M. Fakour, A. Vahabzadeh, D. Ganji, and M. Hatami, "Analytical study of micropolar fluid flow and heat transfer in a channel with permeable walls," *Journal of Molecular Liquids*, vol. 204, pp. 198–204, 2015.

[37] E. Haile and B. Shankar, "Heat and mass transfer through a porous media of MHD flow of nanofluids with thermal radiation, viscous dissipation and chemical reaction effects," *American Chemical Science Journal*, vol. 4, no. 6, pp. 828–846, 2014.

[38] M. Uddin, O. A. Bég, A. Aziz, A. Ismail *et al.*, "Group analysis of free convection flow of a magnetic nanofluid with chemical reaction," *Mathematical Problems in Engineering*, vol. 2015, 2015.

[39] R. A. Damseh, M. Al-Odat, A. J. Chamkha, and B. A. Shannak, "Combined effect of heat generation or absorption and first-order chemical reaction on micropolar fluid flows over a uniformly stretched permeable surface," *International Journal of Thermal Sciences*, vol. 48, no. 8, pp. 1658–1663, 2009.

[40] A. J. Chamkha and A. Rashad, "Unsteady heat and mass transfer by MHD mixed convection flow from a rotating vertical cone with chemical reaction and Soret and Dufour effects," *The Canadian Journal of Chemical Engineering*, vol. 92, no. 4, pp. 758–767, 2014.

[41] K. Das, "Effect of chemical reaction and thermal radiation on heat and mass transfer flow of MHD micropolar fluid in a rotating frame of reference," *International journal of heat and mass transfer*, vol. 54, no. 15-16, pp. 3505–3513, 2011.

[42] S. Ibrahim, P. Kumar, G. Lorenzini, and E. Lorenzini, "Influence of Joule Heating and Heat Source on Radiative MHD Flow over a Stretching Porous Sheet with Power-Law Heat Flux," *Journal of Engineering Thermophysics*, vol. 28, no. 3, pp. 332–344, 2019.

[43] R. W. Fox, A. T. McDonald, and P. Pitchard, "Introduction to fluid mechanics, 2004," 2006.

[44] R. Bansal, *A textbook of fluid mechanics*. Firewall Media, 2005.

[45] S. S. Molokov, R. Moreau, and H. K. Moffatt, *Magnetohydrodynamics: Historical evolution and trends*. Springer Science & Business Media, 2007, vol. 80.

[46] S. K. Das, S. U. Choi, W. Yu, and T. Pradeep, *Nanofluids: science and technology*. John Wiley & Sons, 2007.

[47] H. Schlichting and K. Gersten, *Boundary-layer theory*. Springer, 2016.

[48] D. F. Young, B. R. Munson, T. H. Okiishi, and W. W. Huebsch, *A brief introduction to fluid mechanics*. John Wiley & Sons, 2010.

[49] Y. A. Cengel, *Fluid mechanics*. Tata McGraw-Hill Education, 2010.

[50] H. Chanson, *Applied hydrodynamics: an introduction to ideal and real fluid flows.* CRC press, 2009.

[51] W. M. Rohsenow, J. P. Hartnett, Y. I. Cho *et al.*, *Handbook of heat transfer.* McGraw-Hill New York, 1998, vol. 3.

[52] J. N. Reddy and D. K. Gartling, *The finite element method in heat transfer and fluid dynamics.* CRC press, 2010.

[53] F. M. White and J. Majdalani, *Viscous fluid flow.* McGraw-Hill New York, 2006, vol. 3.

[54] R. W Fox and A. T Mcdonald, "Introduction to flud mechanics," 2004.

[55] J. Kunes, *Dimensionless physical quantities in science and engineering.* Elsevier, 2012.